The Institute of Paper Chemistry

Appleton, Wisconsin

Doctor's Dissertation

The Retention of Fibers from Dilute Suspensions

Richard W. Abrams

June, 1964

LOAN COPY
To be returned to
EDITORIAL DEPARTMENT

THE RETENTION OF FIBERS FROM DILUTE SUSPENSIONS

A thesis submitted by

Richard W. Abrams

B.S. 1959, The University of Notre Dame
M.S. 1961, Lawrence College

in partial fulfillment of the requirements
of The Institute of Paper Chemistry
for the degree of Doctor of Philosophy
from Lawrence College,
Appleton, Wisconsin

June, 1964

Correlation of the Data Using the Method of Single Dimension 70

Experimental Observations 72

Application to Sheet Forming in Practical Systems 75

CONCLUSIONS 79

NOMENCLATURE 81

ACKNOWLEDGMENTS 85

LITERATURE CITED 86

APPENDIX I. DERIVATION OF THE SCAN-LINE RELATIONSHIP 88

APPENDIX II. EXPERIMENTAL DATA 91

APPENDIX III. RELATIVE MAGNITUDES OF FLUID DRAG AND FIBER DEPOSITION FORCES 96

TABLE OF CONTENTS

	Page
SUMMARY	1
INTRODUCTION	2
FACTORS RELEVANT TO THE MECHANISM OF RETENTION	5
Fiber Retention in the Most General Sense	5
Conditions Necessary and Sufficient for Retention in an Idealized System	9
METHODS OF CORRELATING THE FIBER RETENTION PROCESS	14
Direct Method	15
Monte-Carlo Method	17
Network Model Method	20
Nature of the Model for Rectangular-Mesh Networks	26
Nature of the Model for Random Networks	31
Nature of the Model for Networks in General	34
The Empirical Method of Single Dimension	37
EXPERIMENTAL	40
Objectives and General Design of the Retention Experiments	40
The Fiber Retention Apparatus	41
Fibers, Grids, and Other Materials	46
Experimental Procedures	47
Preparatory Procedure	47
Retention Run Procedure	48
Procedure Used in Converting the Mass Data to Standard Form	49
Procedure Used in Network Photograph Analysis	50
RESULTS AND DISCUSSION	51
Presentation and Analysis of the Data in Light of the Network Model	51

SUMMARY

The conditions necessary and sufficient for a fiber to be retained by a relatively open network lying in a plane perpendicular to the direction of fiber movement have been set forth in a general manner. A two-dimensional network model has been developed which allows the determination of the average probability of fulfilling these conditions of retention. The model is based upon the use of a function describing a distribution of network distances which allows a description of the fiber retention process to be made without the necessity of having an explicit description of the network geometry. The validity of the model has been demonstrated by applying it for the case of fiber retention by an ideal rectangular-mesh network. For this simplified case, it was possible to determine the theoretical nature of the distribution of network distances. The model was specifically applied for an ideal system of straight rigid fibers acting as individual units free of the normal interacting factors. An attempt to duplicate this ideal system using a dilute aqueous suspension of nylon fibers was only partially successful. Certain suspension-network interactions were inherently present, and the measured rates of fiber retention were consistently lower than predicted from the model. The network distance distributions used in applying the model were determined from photographs taken of the retaining network as it existed at different stages of the fiber retention process. By applying the network model to the hypothetical case of fiber retention by a random network and empirically describing the functional relationship between the rate of retention and the average network distance, a previously suggested empirical equation was derived. This empirical equation was found to give a good description of the experimental retention curves, and it was suggested that it might be applied to describe the retention process in actual papermaking operations.

INTRODUCTION

Fiber retention is a subject of increasing importance to both the production-oriented papermaker and the scientifically minded researcher. In both instances interest in the subject stems from the same inherent characteristic of the process, the fact that in practical systems fiber retention is seldom complete. To the papermaker the basic problem is essentially no different than it has always been; complete retention must be sacrificed in order to obtain the required drainage and such side effects as two-sidedness must be accepted as the consequence. His increased interest is predominantly the result of increased production demands. The interest of the researcher, on the other hand, has been given new meaning in recent years as studies on the structure of paper have focused upon development of the theory of structure (1-10). His interest is now not so much with such secondary effects as two-sidedness as with the nature of the variation in the internal sheet structure which causes these secondary effects. Incomplete retention is one of the causes of this variation in structure. As the sheet builds up, retention, particularly of fines, fillers, and short fibers, increases causing a variation in structure across the thickness of the sheet. The extent of this variation can be reduced by increasing retention, but not without influencing the co-processes of dispersion and drainage (11-12). If retention is increased through an increase in the consistency of the feed, the tendency for flocculation, which is itself the source of another type of variation in sheet structure, is also increased. If retention is increased by using a smaller mesh wire, the rate of drainage must necessarily be decreased. In practice, therefore, determination of the proper combination of retention, dispersion, and drainage presupposes some knowledge of all three processes. Understanding of the complex sheet-forming process can thus be considerably advanced by

studying each of these individual processes in idealized systems where they are effectively isolated from the major influences of the others. To study retention aside from dispersion and drainage, however, still involves the essentially different processes of fiber retention and fines and filler retention. For this reason, it is expedient to further isolate the process of fiber retention from that of fines and filler retention. Studies of such isolated systems have already supplied extensive information regarding the mechanisms involved. The retention of fines and fillers has been shown to depend upon several distinct mechanisms (13). The retention of fibers, on the other hand, has been found to depend primarily upon the single mechanism of mechanical interception (14-18). Knowing the nature of this mechanism, it is now desirable to know how it is dependent upon sheet structure, or in other words, in what manner does the increase in fiber retention with basis weight depend upon the change in structure. To know this is to know how that portion of the variation in sheet structure caused by a continuous variation in the distribution of fiber lengths is related to the basic process of incomplete fiber retention.

One of the characteristics of a fiber is that it has a high axis ratio, that is, its length is many times greater than any dimension of its cross section. Insofar as fibers are concerned, this characteristic is largely accountable for the occurrence of incomplete retention. Consider, for example, one opening of a wire cloth. A fiber will be retained by this opening only if it is oriented such that it can bridge across the opening. A fiber not so oriented upon approaching the opening will pass through unretained. Whether or not a particular orientation will result in retention depends upon the geometry of the opening and upon the effective dimensions of the fiber (14). These, in turn, may be influenced by such factors as the hydrodynamic field existing around the opening and the

interactions which take place with other particles in the approaching suspension (14-17). Recognizing the dependence of fiber retention upon the properties of the fibers and the wire grid, the hydrodynamic field, and the interactions between fibers, Estridge (14) developed generalized expressions describing fiber retention in terms of a probability function which is also dependent upon these factors. He then demonstrated the validity of the approach by applying this probability function under a restricted set of conditions for the case of the initial retention of fibers by bare wires. In his work, he depended upon the direct integration of the probability function to evaluate the retention probability. Nelson (19) has since demonstrated that the retention probability can be evaluated by means other than direct integration. He has determined the probability of fiber retention by rectangular grids, under the same set of restricted conditions employed by Estridge, by statistically evaluating the probability function through multiple random trial. Both of these methods of evaluating the retention probability function require an explicit description of the geometry of the retaining network. For this reason, it is virtually impossible to apply them much beyond the stage of initial retention. The objective of the present work has been to eliminate the need for this explicit description of the geometry, either through an evaluation of the retention probability function by a method which does not require such a description or through the use of an empirical correlation which does not require evaluation of the retention probability function. This makes it possible to predict the probability of fiber retention by the fiber-wire networks which exist beyond the stage of initial retention.

FACTORS RELEVANT TO THE MECHANISM OF RETENTION

FIBER RETENTION IN THE MOST GENERAL SENSE

To predict whether or not a single fiber will be retained by a relatively open network such as a wire grid, requires information not readily obtainable in actual systems. Given sufficient details of the process, however, it is possible to estimate what fraction of a large sample of fibers will be retained.

Consider a fluid suspension of j types of fibers flowing in the negative Z direction toward a retaining network of area A located in the X-Y plane. Let N_i be defined as the number of ith-type fibers approaching the differential area $dxdy$. The probability that this type of fiber will be retained is P_i, expressed as the ratio of retained fibers to total fibers of the ith type. The probability P_i is an average value dependent upon the distribution of approaching fiber orientations. The number of ith-type fibers retained, n_i, over the area A is then

$$n_i = (1/A) \int \int P_i N_i dxdy \qquad (1).$$

A summation for all j types of fibers gives the total number of fibers retained over the area A:

$$n_t = (1/A) \sum_{i=1}^{j} \int \int P_i N_i dxdy \qquad (2).$$

If the number of approaching fibers is independent of x and y, Equation (1) reduces to

$$n_i = (1/A) N_i \int \int P_i dxdy = \overline{P}_i N_i \qquad (3),$$

where $\bar{P}_i$ is the average retention probability of the ith-type fiber over the area A.

It is normally more convenient to deal with the fiber mass than with the number of fibers. If the mass per fiber of the ith type is σ_i and if the average fiber mass for all j types of retained fibers is $\bar{\sigma}_r$, the mass equivalent of Equation (2) combined with Equation (3) is

$$\bar{\sigma}_r n_t = \sum_{i=1}^{j} \sigma_i \bar{P}_i N_i \qquad (4).$$

The rate of retention (the rate of change of the mass of fibers retained with respect to the total approaching mass of fibers) can now be defined as the fraction R retained from the total approaching mass of fibers, dW_t,

$$R = dW_r/dW_t = (1/\bar{\sigma}N_t) \sum_{i=1}^{j} \sigma_i \bar{P}_i N_i \qquad (5),$$

where dW_r is the mass of fibers retained, N_t is the total number of approaching fibers, and $\bar{\sigma}$ is the average fiber mass for all j types of approaching fibers. The rate of retention can thus be evaluated from a knowledge of the average retention probability, $\bar{P}_i$.

Each of Equations (1) through (5) is an expression of the dependence of fiber retention upon the probability function as employed by Estridge. According to Equation (1), fiber retention is a function of the product $P_i N_i$ and of the manner in which this product varies over the area of the retaining medium. Variation in the product $P_i N_i$ can in general be attributed to variations within the approaching suspension, to variations within the retaining network, or to variations caused by suspension-network interactions. Variations within the

suspension include the distribution of fiber centers and the distribution of fiber orientations. These in turn are dependent upon the fiber concentration, the degree of fiber-fiber interaction or flocculation, and the degree of fiber-fluid interaction or the hydrodynamics of the suspension. Variations within the retaining network are directly associated with the geometric structure of the network. Variations caused by suspension-network interactions include changes in the hydrodynamics of the suspension due to the presence of the network, changes in the network structure due to fluid drag forces, and changes in the network structure or in the positions of fibers relative to the network due to friction and impact forces which occur as fibers come into contact with the network. Evaluation of the general fiber retention probability function, $\underline{P}_i \; \underline{N}_i$, requires a knowledge of the nature and interdependence of all these factors. This would require a level of understanding much beyond what is presently available. It is possible, however, to advance the level of present understanding by considering the influence of but one or two of these factors upon the retention probability. This can be accomplished through the study of an idealized system under a restricted set of conditions. The value of such an approach in the analysis of complex phenomena has long been recognized and has, in fact, been demonstrated in this particular area by the work of Estridge and Nelson. A similar approach was used in the experimental portion of this work.

The rate of fiber retention as expressed by Equation (5) implies the restricting condition that the number of approaching fiber centers is uniform with respect to area. From this equation, it is seen that if the cumulative mass of fibers retained, $\underline{W}_r$, is plotted as a function of the total mass of fibers that have approached the retaining network, $\underline{W}_t$, as in Fig. 1, the rate of fiber retention at any point is given by the slope. The initial slope of

such a curve must be finite. This initial slope is what Estridge termed the initial retention. As the total mass of fibers increases, the rate of retention also increases because of a continuous closing of the structure of the retaining network. The structure eventually closes to the point where fiber retention is complete and the slope of the curve is equal to unity. The total mass of fibers which has passed unretained, $\underline{W}_p$, is equal to the value of $\underline{W}_t$ determined by extending the unit slope portion of the retention curve to $\underline{W}_r = 0$. If more than one type of fiber is present, the rate of retention at any point in the process will vary from one type to another unless the respective rates are equal to unity. The distribution of fiber types in the network is thus a function of the distribution in the approaching suspension and of the relative rates of retention. Once the unit slope portion of the curve is attained, the individual retention rates are all identical and the composition of further deposition is the same as that of the approaching suspension. Up to this point, however, network structure is dependent upon the nature of the fiber retention process.

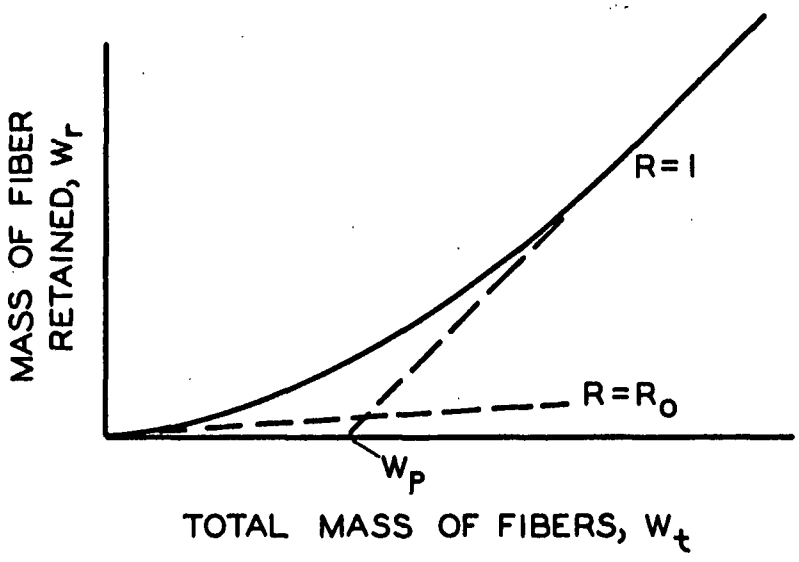

Figure 1. Fiber Retention Curve

CONDITIONS NECESSARY AND SUFFICIENT FOR RETENTION IN AN IDEALIZED SYSTEM

In an idealized system of straight, rigid fibers, the probability of retention is dependent upon the dimensions and orientations of the fibers, the dimensions of the network, and the manner in which the fibers behave upon reaching the network. Fiber orientation can be specified by two angles, the co-latitude θ, or the angle the fiber makes with the positive $\underline{Z}$-axis, and the azimuth ϕ or the angle the fiber's $\underline{x}$-$\underline{y}$ projection makes with the positive $\underline{X}$-axis. This is illustrated in Fig. 2. The fiber's location can be specified by the co-ordinates of its midpoint $(\underline{x}_c, \underline{y}_c, \underline{z}_c)$. The network dimensions can be specified by one angle and two distances, the angle being ϕ measured from the positive $\underline{X}$-axis, and the distances being λ_1 and λ_2 measured from the point $(\underline{x}_c, \underline{y}_c)$ to the first crossing of a member of the network in the $(\phi + \pi)$ and ϕ directions, respectively. This is illustrated in Fig. 3. Estridge found that in a system in which there is no interaction between fibers within the suspension it is valid to assume that for a short distance above the retaining network the fiber moves in the negative $\underline{Z}$ direction without change in the value of $(\underline{x}_c, \underline{y}_c)$ and further, that upon contact with the network, the fiber rotates without change in the value of $(\underline{x}_c, \underline{y}_c)$, either until it is retained or until it passes unretained to the downstream side of the network. If it is also assumed that the network structure is not altered under the impact of the depositing fiber, the conditions necessary and sufficient for retention to occur are:

for $0 \leq \theta \leq \pi/2$,

$$(L_f/2)\sin(\theta) \geq \lambda_1, \quad \text{and} \quad (L_f/2) \geq \lambda_2,$$

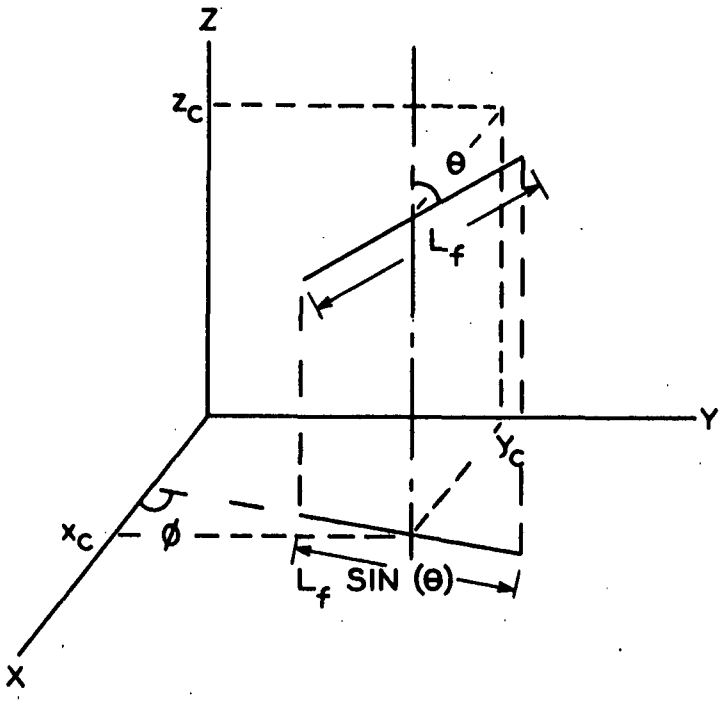

Figure 2. Fiber Orientation

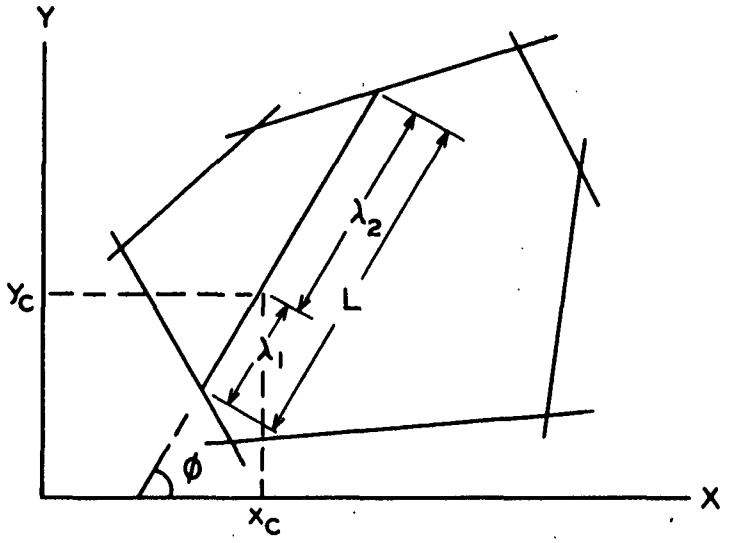

Figure 3. Dimensions of Retaining Network

for $\pi/2 \leq \theta \leq \pi$,

$$(L_f/2)\sin(\theta) \geq \lambda_2, \quad \text{and} \quad (L_f/2) \geq \lambda_1,$$

where L_f is the fiber length. For reasons of symmetry, it is sufficient to consider merely the first set of conditions in which θ varies from 0 to $\pi/2$. Letting $S = \sin(\theta)$ and defining the distance L as the summation of λ_1 and λ_2, the conditions necessary for retention are:

$$2\lambda_1/L_f \leq S \tag{6}$$

$$2L/L_f - 1 \leq S \tag{7}.$$

The probability of retention for a large number of straight, rigid fibers can now be evaluated from a knowledge of the variation in L_f, θ, ϕ, (x_c, y_c), λ_1, and L. For a given length fiber and a given value of (x_c, y_c), evaluation of the above conditions for all possible values of θ, ϕ, λ_1, and L constitutes evaluation of P_i. It is convenient to introduce the variable p as an expression of whether a fiber having a particular location and orientation will or will not be retained. By definition, if the conditions of Equations (6) and (7) are satisfied, p is equal to unity; if they are not satisfied, p is equal to zero. Evaluation of P_i then involves a determination of the average value of p for all values of the independent variables θ and ϕ.

In essence, the above conditions for retention state that in order to be retained a fiber must be supported at least one point on each side of its center. This is in agreement with Estridge's analysis. It is possible, however, for a fiber to be retained without the existence of support to one side of its center. This possibility is the result of a tucking-under process in which rotation brings the lower end of the fiber back up into contact with the underside of

the retaining network, such as depicted in Fig. 4. The fiber is then retained in a cantilever position. Although this possibility is admitted, and has in fact been observed, its contribution to the retention process is neglected in this work. No attempt has been made to determine quantitatively the validity of this neglect, but for retention by relatively open networks other than the bare wire, this assumption has been qualitatively observed to be much less serious than the assumption that there is no structural rearrangement of the network under fiber impact. This is discussed in more detail below.

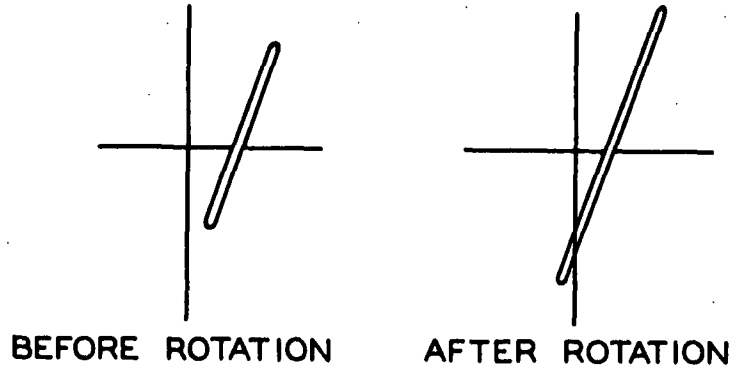

Figure 4. Fiber Retention by Cantilever Support

If, in addition to the limitations imposed above, it is assumed that each type of fiber is distributed randomly throughout the suspension both with regard to position and orientation, then evaluation of the retention probability can be greatly simplified. Randomness with respect to position implies that all values of $(\underline{x}_c, \underline{y}_c)$ are equally probable. Randomness with respect to orientation will here be defined to mean that the end points of a fiber occupy with equal probability any of a large number of points which are distributed uniformly over the surface of the sphere whose center coincides with the fiber mid-point and whose diameter is equal to the fiber length. Fiber orientation is random in this sense if ϕ is distributed uniformly between 0 and 2π and if the distribution of

θ between 0 and $\pi/2$ is proportional to the sine of θ and independent of ϕ. Symmetry here again permits consideration of only a portion of the total range. The only additional information required to evaluate the conditions for retention from a suspension of randomly distributed fibers is the nature of the variation in $\underline{L_f}$, λ_1, and $\underline{L}$. Variation with respect to fiber lengths is in direct proportion to their number and can be treated by adding together the contributions of the different lengths as in Equations (2) and (5). Variation in λ_1 and $\underline{L}$ is dependent upon the structure of the retaining network and can be treated in different ways. The means of describing the variation in λ_1 and $\underline{L}$ and the corresponding methods of evaluating the conditions necessary and sufficient for retention are dealt with below. The systems to be discussed are all governed by the restricting conditions set forth in this section.

METHODS OF CORRELATING THE FIBER RETENTION PROCESS

There are two general approaches which can be taken in predicting the rate of fiber retention as a function of the characteristics of the bare wire and the amount of fibers already retained. The retention probability $\underline{P_i}$ can be evaluated theoretically by a complete analysis of the variables set forth in the preceding section, and the rate of retention can then be found from Equations (3) and (5), or the rate of retention can be predicted directly from an empirical correlation founded upon the results of prior experimentation. The theoretical approach is by its very nature more fundamental and more descriptive of the actual mechanism of fiber retention. The empirical approach, on the other hand, may be of much greater value in describing the over-all results. This would be true particularly if it were beyond the scope of available knowledge to make a complete theoretical analysis. Both approaches have obvious value. Any particular method of correlating the fiber retention process must follow one of these two approaches or some hybrid combination of them. Of the four methods discussed in this section, three have theoretical foundations; the other has an empirical foundation. One method, that of Estridge, is strictly a theoretical treatment. Another method, one which is herein referred to as that of the Network Model, can be strictly theoretical but derives its greatest value from its basic ability to combine with an empirical evaluation. The Monte-Carlo Method, or Nelson's method of multiple random trial, has the same theoretical basis as Estridge's method but involves the empirical evaluation of the retention probability through a statistical process of multiple trial. The Empirical Method of Single Dimension is the only method discussed which has a basically empirical foundation. Even this method, however, can be partially connected with theory.

The systems discussed under each of the four methods are governed by the restrictions set forth in the previous section. These are: that the suspensions be composed of straight, rigid fibers and be dilute enough so that fiber-fiber interaction will be negligible, that the flow patterns be such that the fibers will be randomly distributed both with respect to position and orientation, that there be no appreciable interaction between the suspension and the retaining network, and that upon contacting the network the fibers rotate without change in the ($\underline{x}$, $\underline{y}$) co-ordinates of their centers. Although all four correlation methods are applicable to systems containing multiple fiber lengths, they have been applied specifically only for systems containing essentially one fiber length. Such limited application is sufficient to demonstrate the general validity of each method and greatly simplifies discussion as well as experimental verification.

DIRECT METHOD

It is not the intent here to treat Estridge's method in great detail but only to outline the general approach which he employed. This can be done by considering whether a fiber having a particular orientation and location will or will not be retained by a square-mesh grid and then indicating how Estridge extended the analysis to determine the rate of initial retention. Consider, for example, the particular case where the values of ($\underline{x}_c$, $\underline{y}_c$) and ϕ are such that the distance $\underline{L}$ is measured across one corner of the square of Side $\underline{a}$, as shown in Fig. 5. λ_1 and ($\underline{L}$-λ_1) are then equal to $-\underline{y}_c/\sin(\phi)$ and $-\underline{x}_c/\cos(\phi)$, respectively. Knowing the value of θ, it can be ascertained whether $\underline{p}$ is equal to 0 or 1 from a consideration of Equations (6) and (7). Figure 6 illustrates another case involving the same values of $\underline{x}_c$ and $\underline{y}_c$ but a different value of ϕ.

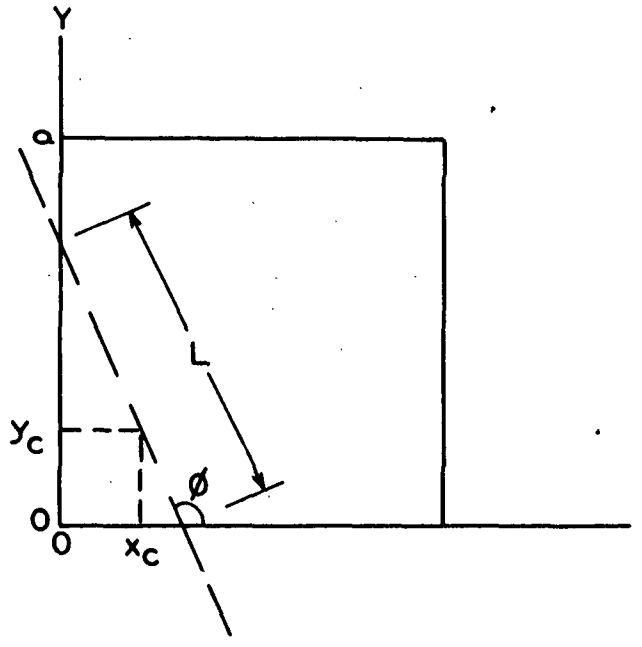

Figure 5. Illustration of Dependence of $\underline{L}$ on $\underline{x_c}$, $\underline{y_c}$, and Ø

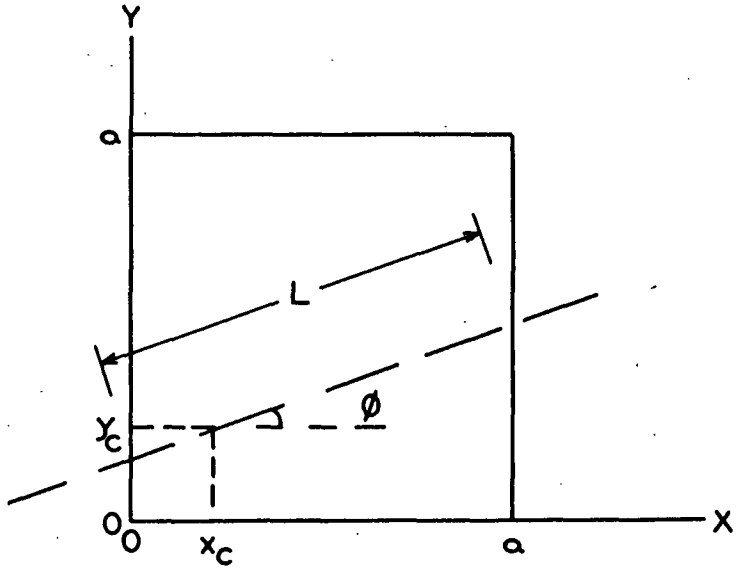

Figure 6. Second Illustration of the Dependence of $\underline{L}$ on $\underline{x_c}$, $\underline{y_c}$, and Ø

In this case, λ_1 and $(\underline{L}-\lambda_1)$ are equal to $\underline{x}_c/\cos(\emptyset)$ and $(\underline{a}-\underline{x}_c)/\cos(\emptyset)$, respectively. Again, $\underline{p}$ can be determined if θ is known.

These two particular cases have been picked to illustrate two separate regions of integration for $\emptyset$. Essentially, what Estridge did was to define all the possible regions of integration in terms of the dimensions of the grid and then to determine the average value of $\underline{p}$, for all θ and $\emptyset$, as a function of $\underline{x}_c$ and $\underline{y}_c$. The average retention probability can then be determined by combining Equations (3) and (5) and integrating with respect to $\underline{x}_c$ and $\underline{y}_c$. For a system containing a single type of fiber, the rate of retention is equal to the average retention probability. According to Equation (3), the rate of retention is, therefore,

$$R = \overline{P}_i = (1/A) \int \int P_i dxdy \qquad (8).$$

Estridge's method thus involves an exact theoretical evaluation of the equations defining the fiber retention process. Its usefulness in predicting the rate of retention in physical systems is limited only by the restrictions which it has been necessary to impose in order to evaluate the general probability function and by the ability to define the functional relationships between θ, $\emptyset$, $\underline{x}_c$, and $\underline{y}_c$. It can be readily seen that for systems in which the retaining network has any but the most simple geometric configuration, defining the necessary functional relationships between θ, $\emptyset$, $\underline{x}_c$, and $\underline{y}_c$ is virtually impossible. In practice, therefore, evaluations employing this method have been limited to determinations of the rate of initial retention.

MONTE-CARLO METHOD

As mentioned before, the basic approach employed by Nelson is identical to that used by Estridge. Nelson, however, circumvents the need for defining the

general functional relationships between θ, ϕ, x_c, and y_c by evaluating numerous specific cases such as those illustrated above. The particular cases to be evaluated are selected randomly by a Monte-Carlo-type process. Specifically, four random numbers are required to define the conditions in each case or trial. The four random numbers T_1, T_2, T_3, and T_4 are each distributed independently and uniformly on the interval between and including 0 and 1. The average retention probability is then determined in the following manner.

Consider a rectangular grid of sides a and b, ($b \geq a$), located in the x-y plane such that parallel wires are located at $x = 0$, $x = \pm a$, $x = \pm 2a$.... and at $y = 0$, $y = \pm b$, $y = \pm 2b$.... For reasons of symmetry, it is sufficient to consider one quarter of one rectangular mesh. The values of the four independent variables, x_c, y_c, θ, and ϕ, which define the conditions of each trial, are selected according to the relationships

$$x_c = (a/2)T_1 \qquad (9),$$

$$y_c = (b/2)T_2 \qquad (10),$$

$$\theta = \arccos(1 - T_3) \qquad (11),$$

$$\phi = 2\pi T_4 \qquad (12),$$

It is immediately apparent that x_c, y_c, and ϕ vary according to their prescribed patterns. For the distribution of θ between 0 and $\pi/2$ to be proportional to the sine of θ is to say that the frequency with which values of the angle θ fall within a small interval $\Delta\theta$ containing θ is proportional to $\sin(\theta)\Delta\theta$. It can be shown that the random distribution determined by Equation (11) meets this requirement.

In each trial, values of x_c, y_c, θ, and ϕ are selected randomly according to Equations (9) through (12) and the value of p determined from a consideration of

Equations (6) and (7). The values of λ_1 and L are determined in each trial in a manner similar to that given in the examples of the preceding section. The average retention probability is then given by

$$P_i = (1/N) \sum^{N} p = n/N \qquad (13),$$

where N is the total number of trials and n is the number of trials resulting in retention. The accuracy of $\bar{P}_i$ determined in this manner will vary depending upon the total number of trials. It is thus necessary to consider the statistics of such a series of trials.

If an event is known to have the probability P, the probability that n successes will result when N trials are made without bias is given by the binomial distribution (20),

$$F(n) = \{N!/[n!(N - n)!]\} P^N(1 - P)^{N-n} \qquad (14).$$

The expectation value of n is

$$\bar{n} = PN \qquad (15),$$

and the variance is

$$\overline{(n - \bar{n})^2} = P(1 - P)N \qquad (16).$$

In successive experiments of the same total number of trials, the estimate of $\bar{P}_i$ obtained from Equation (13) will differ from the correct value P to the extent indicated by the standard deviation,

$$[\overline{(n - \bar{n})^2}]^{1/2}/N = [P(1 - P)/N]^{1/2} \qquad (17).$$

This quantity is seen to be a slowly decreasing function of $\underline{N}$. If it is required that the standard deviation of the estimate shall not exceed 0.5×10^{-2} at any point in the range of $\underline{P}$, then it is required that $\underline{N} \geq 10^4$. To reduce the standard deviation such as not to exceed 0.5×10^{-3}, however, requires that $\underline{N} \geq 10^6$. That moderate accuracy is achieved easily but that more precise results require a rapidly increasing number of trials is characteristic of Monte-Carlo methods.

Nelson employed this method to determine the rate of initial retention by rectangular-mesh grids. The work was carried out on a digital computer using a total number of trials of 10^4 and using four pseudorandom number generators to determine the values of $\underline{T}_1$, $\underline{T}_2$, $\underline{T}_3$, and $\underline{T}_4$. The rates of initial retention so determined agree closely with those found by Estridge for square- and parallel-mesh grids. Values of the initial retention probability as determined by this method for rectangular grids of Side Ratios 1, 2, and 5 are given in Table I. Although the application of this method in most instances is far simpler than that of Estridge's method, the need of explicitly defining the geometry of the retaining network still imposes a severe limitation.

NETWORK MODEL METHOD

The need for an explicit description of the geometry of the retaining network limits the application of both Estridge's and Nelson's methods to the stage of initial retention. It is feasible to apply Nelson's method to predict the rate of retention when the network consists of the wire grid and a few scattered fibers. As the number of retained fibers increases, however, the volume of calculations required rapidly exceeds present capabilities of performing them. This is due in part to the complex geometry of a fiber-wire network. More important,

TABLE I

PROBABILITY OF INITIAL FIBER RETENTION BY A RECTANGULAR GRID—VALUES DETERMINED USING MONTE-CARLO METHOD

	b/a			
a/L_f	1.0[a]	1.0	2.0	5.0
0.1		0.995	0.987	0.964
0.18	0.97			
0.2		0.974	0.945	0.809
0.26	0.95			
0.3		0.942	0.819	0.674
0.36	0.91			
0.4		0.878	0.646	0.540
0.5		0.737	0.465	0.378
0.6		0.528	0.305	0.228
0.7		0.363	0.194	0.128
0.71	0.41[b]			
0.8		0.243	0.130	0.071
0.9		0.163	0.088	0.037
1.0	0.12	0.121	0.068	0.023
1.1		0.101	0.053	0.019
1.2	0.09	0.088	0.042	0.016
1.4	0.06	0.062	0.030	0.012

[a]This column contains the square-mesh data of Estridge (14).

[b]This value appears to be in error.

however, is the fact that because fiber retention is a chance phenomenon, the position of a given number of fibers is also a matter of chance. Thus, although the process can always be simulated using the Monte-Carlo method, the number of trials required becomes exceedingly large. The objective of this work has been to extend analysis of the fiber retention process beyond the initial stage by eliminating the need for this explicit description of the network geometry. The Network Model provides one method by which this can be accomplished.

The conditions necessary and sufficient for a fiber to be retained are given by Equations (6) and (7). The dependence of fiber retention upon the geometry of the retaining network is represented in these equations by the distances λ_1 and $\underline{L}$. To say that the methods of Estridge and Nelson require an explicit description of the network geometry is merely another way of saying that λ_1 and $\underline{L}$ must be determined for each particular network as explicit functions of the independent variables $\underline{x}_c$, $\underline{y}_c$, and $\emptyset$. For a fiber approaching a particular network with a particular orientation and location, λ_1 and $\underline{L}$ are directly dependent upon $\underline{x}_c$, $\underline{y}_c$, and $\emptyset$. In determining the average retention probability, however, it is just as meaningful to introduce probability density functions for λ_1 and $\underline{L}$ as to introduce such functions for $\underline{x}_c$, $\underline{y}_c$, and $\emptyset$. That this is actually done is the essential characteristic of the Network Model. The reasoning involved in doing this can perhaps be better understood by again considering how λ_1 and $\underline{L}$ are determined in each individual trial of Nelson's Monte-Carlo method. Values of $\underline{x}_c$, $\underline{y}_c$, and $\emptyset$ are selected randomly according to the relationships of Equations (9), (10), and (12). To say that $\underline{x}_c$ is selected properly by a random evaluation of Equation (9) is to say that the random distribution determined from this equation meets the requirement that the frequency with which values of $\underline{x}_c$ fall within a small interval $\Delta\underline{x}$ containing $\underline{x}_c$ be

proportional to $\Delta\underline{x}$. A similar statement can be made regarding the selection of $\underline{y_c}$ and $\emptyset$ by Equations (10) and (12). Having determined values of $\underline{x_c}$, $\underline{y_c}$, and $\emptyset$ in each trial, the values of λ_1 and $\underline{L}$ are determined from the known network geometry. If the dependence upon $\underline{L}$ of the frequency with which values of the distance $\underline{L}$ fall within a small interval $\Delta\underline{L}$ containing $\underline{L}$ were known, and if the nature of the frequency distribution function of λ_1 were also known, then it would no longer be necessary to treat these distances as dependent variables. It is readily apparent that an evaluation of the average retention probability made from a knowledge of the frequency distribution functions for λ_1 and $\underline{L}$ is far less complicated than the same evaluation made from a knowledge of the dependence of λ_1 and $\underline{L}$ on $\underline{x_c}$, $\underline{y_c}$, and $\emptyset$. Take, for example, the case where the retaining network consists of the wire grid and a few fibers. It is no longer necessary to know the exact position of these fibers since the probability density functions of λ_1 and $\underline{L}$ which are representative of the network at this stage in the retention process are not dependent upon the precise location of each fiber. A further simplification stems from the fact that, by definition, λ_1 must be less than or equal to $\underline{L}$. λ_1 is then dependent upon $\underline{L}$, and the only independent variable connected with the structure of the retaining network is $\underline{L}$.

In addition to the frequency distribution functions of $\underline{L}$, and λ_1 given $\underline{L}$, the network model employs a probability density function for the angle θ, or for some function of this angle. When dealing with randomly oriented fibers, it is convenient to use the distribution of the sine of θ. For the frequency with which values of the angle θ fall within a small interval $\Delta\theta$ containing θ to be proportional to $\sin(\theta)\Delta\theta$, the probability density function of $\underline{S}$ must be

$$F(S) = S(1 - S^2)^{-1/2} \qquad (18).$$

It now remains to consider the nature of the frequency distribution functions of $\underline{L}$, and λ_1 given $\underline{L}$, and the manner in which the average retention probability is dependent upon these two distributions and the distribution of $\underline{S}$.

From the definitions of λ_1 and $\underline{L}$, it follows that λ_1 must be less than or equal to $\underline{L}$, and, to satisfy the conditions of Equation (6), λ_1 must be less than or equal to $\underline{L_f}/2$. For retention to occur, therefore, λ_1 must satisfy the following limits:

$$\text{for } 0 \leq L \leq L_f/2, \qquad 0 \leq \lambda_1 \leq L \qquad (19),$$

$$\text{for } L_f/2 \leq L \leq L_f, \qquad L - L_f/2 \leq \lambda_1 \leq L_f/2 \qquad (20).$$

To satisfy the conditions of Equation (7), $\underline{L}$ must be less than or equal to $\underline{L_f}$. Then if the frequency distribution of $\underline{L}$ is $\underline{F}(\underline{L})$ and the conditional frequency distribution of λ_1 given $\underline{L}$ is $\underline{F}(\lambda_1 | \underline{L})$, the average retention probability is

$$\overline{P}_i = \int_0^{L_f/2} F(L) \int_0^{L} F(\lambda_1 | L) \int_{2\lambda_1/L_f}^{1} F(S)\,dS\,d\lambda_1\,dL + \int_{L_f/2}^{L_f} F(L) \int_{L-L_f/2}^{L_f/2} F(\lambda_1 | L) \int_{2\lambda_1/L_f}^{1} F(S)\,dS\,d\lambda_1\,dL \qquad (21).$$

In other words, $\overline{P}_i$ is simply the ratio of all the combinations of λ_1, $\underline{L}$, and $\underline{S}$ which will result in the retention of a fiber of length $\underline{L_f}$ to the total number of combinations of λ_1, $\underline{L}$, and $\underline{S}$.

The nature of the distribution function $\underline{F}(\lambda_1 | \underline{L})$ follows directly from the definitions of the network distances λ_1 and $\underline{L}$. For a given value of $\underline{L}$, the frequency with which values of λ_1 fall within a small interval $\Delta\lambda_1$ containing λ_1 is proportional to $\Delta\lambda_1$. Therefore, the conditional distribution of λ_1 given $\underline{L}$ is rectangular, or of constant frequency $\underline{B_L}$, as illustrated in Fig. 7 and

described by

$$F(\lambda_1|L) = B_L \qquad (22).$$

Combining this with Equation (21) and integrating gives the average retention probability as a function of $\underline{L}$ and $\underline{F}(\underline{L})$:

$$\bar{P}_i = (B_L/L_f)\int_0^{L_f/2} F(L)[L(L_f^2/4 - L^2)^{1/2} + (L_f^2/4)\arcsin(2L/L_f)]dL$$

$$+ (B_L/L_f)\int_{L_f/2}^{L_f} F(L)\left\{\pi L_f^2/8 + (L_f/2 - L)(LL_f - L^2)^{1/2}\right.$$

$$\left. + (L_f^2/4)\arcsin[(L_f - 2L)/L_f]\right\} dL \qquad (23).$$

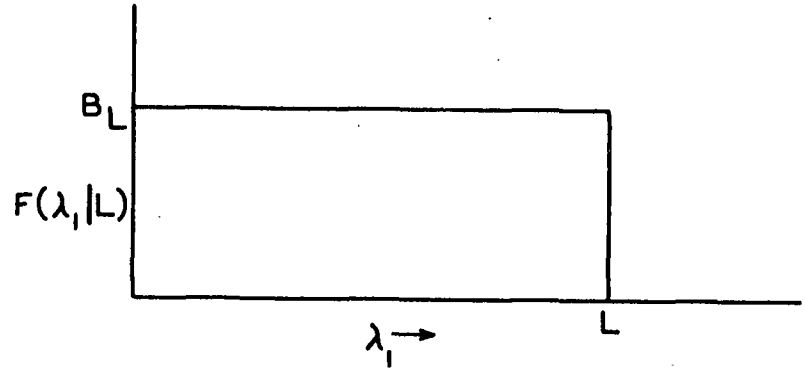

Figure 7. Conditional Frequency Distribution of λ_1 Given $\underline{L}$

The nature of the frequency distribution of $\underline{L}$ is dependent upon the general structural characteristics of the retaining network. Two specific types of networks and the corresponding $\underline{L}$ distributions are discussed below. The only thing which can be said of the distribution of $\underline{L}$ in general is that the frequency with which values of $\underline{L}$ fall within a small interval $\Delta\underline{L}$ must necessarily be a never-increasing function of $\underline{L}$ except at values of $\underline{L}$ where the distribution is

discontinuous. That this must be true will become more apparent from the discussion of the specific types of network.

NATURE OF THE MODEL FOR RECTANGULAR-MESH NETWORKS

Consider a rectangle having sides of lengths $\underline{a}$ and $\underline{b}$ where $\underline{a}$ is less than or equal to $\underline{b}$. The frequency distribution of $\underline{L}$ can be determined by passing a set of parallel lines, equally spaced in the $(\phi + \pi/2)$ direction, across the rectangle in the direction ϕ, and then repeating this procedure using the same spacing for all angles ϕ uniformly distributed from 0 to $\pi/2$ (Fig. 8). The distance $\underline{L}$ is measured along each line from the point at which it enters the rectangle to the point at which it leaves the rectangle.

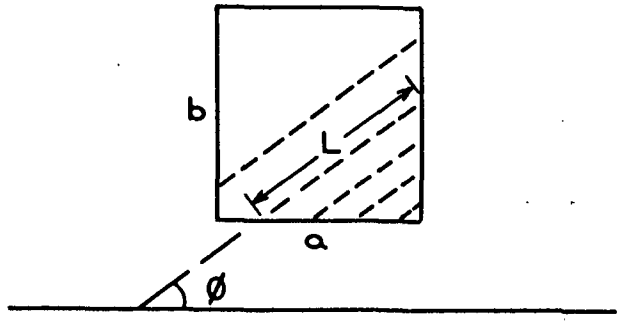

Figure 8. Analysis of Rectangle for Distance $\underline{L}$

When ϕ is less than $\arctan(\underline{b}/\underline{a})$ as shown in Fig. 8, there is a continuous distribution of the distance $\underline{L}$ for $0 \leq \underline{L} \leq \underline{a}/\cos(\phi)$, but a concentration of distances at $\underline{L}$ equal to $\underline{a}/\cos(\phi)$. Thus, for ϕ less than or equal to $\arctan(\underline{b}/\underline{a})$, the distribution of $\underline{L}$ is as shown in Fig. 9, where the ratio of the knob area, (symbolic of an ideally concentrated frequency of $\underline{L}$), to the total area is

$$[b \cos(\phi) - a \sin(\phi)]/[b \cos(\phi) + a \sin(\phi)].$$

When ϕ is greater than or equal to $\arctan(b/a)$, the distance having concentrated density is $b/\sin(\phi)$ and the ratio of the knob area to the total area is

$$[a \sin(\phi) - b \cos(\phi)]/[a \sin(\phi) + b \cos(\phi)].$$

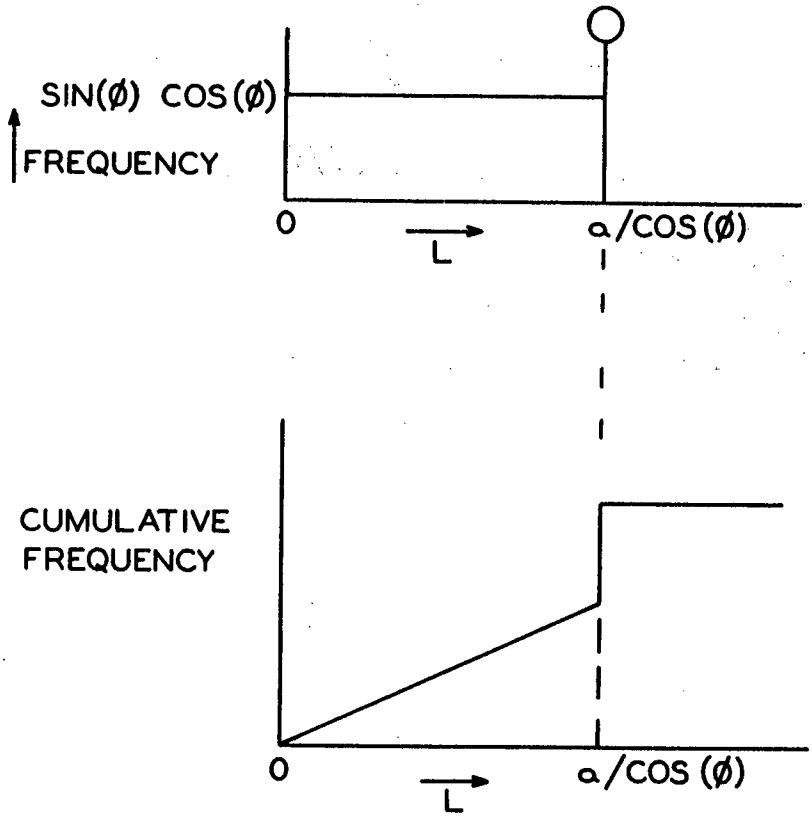

Figure 9. Distribution of L for $\phi \leq \arctan(b/a)$

The frequency of L for any length $0 \leq L \leq (a^2 + b^2)^{1/2}$ is then obtained by adding together the contributions corresponding to the rectangular areas and those corresponding to the knob areas. Before this can be done, however, it is necessary to introduce a change of variable so that the concentrated frequencies represented by the knobs can properly be taken into account. This change in variable is accomplished through the use of the delta function which represents symbolically an ideally concentrated quantity (21). For $\phi \leq \arctan(b/a)$, a concentrated frequency of $[b \cos(\phi) - a \sin(\phi)]/2$ occurs at a distance of

$\underline{L} = \underline{a}/\cos(\phi)$. Letting γ equal $\underline{L} - \underline{a}/\cos(\phi)$, the proper change of variable is obtained according to the equality

$$[L - a/\cos(\phi)]d\phi = (1/a)\,\delta(\gamma)[\cos^2(\phi)/\sin(\phi)]d\gamma \qquad (24).$$

The corresponding relationship for $\arctan(\underline{b}/\underline{a}) \leq \phi$ is given by the equality

$$[L - b/\sin(\phi)]d\phi = (1/b)\,\delta(\alpha)[\sin^2(\phi)/\cos(\phi)]d\alpha \qquad (25),$$

where α is equal to $\underline{L} - \underline{b}/\sin(\phi)$.

The six possible contributions, $\underline{C}_1$ to $\underline{C}_6$, to the frequency distribution of $\underline{L}$ are, therefore,

For $\underline{L} \leq \underline{a}$,

$$C_1 = \int_0^{\arctan(b/a)} \sin(\phi)\cos(\phi)d\phi = (1/2)[b^2/(a^2 + b^2)] \qquad (26).$$

For $\underline{L} \geq \underline{a}$,

$$C_2 = \int_{\arccos(a/L)}^{\arctan(b/a)} \sin(\phi)\cos(\phi)d\phi = (1/2)[b^2/(a^2 + b^2) - (L^2 - a^2)/L^2] \qquad (27).$$

For $\underline{L} \leq \underline{b}$,

$$C_3 = \int_{\arctan(b/a)}^{\pi/2} \sin(\phi)\cos(\phi)d\phi = (1/2)[1 - b^2/(a^2 + b^2)] \qquad (28).$$

For $\underline{L} \geq \underline{b}$,

$$C_4 = \int_{\arctan(b/a)}^{\arcsin(b/L)} \sin(\phi)\cos(\phi)d\phi = (1/2)[b^2/L^2 - b^2/(a^2 + b^2)] \qquad (29).$$

For $\underline{L} \geq \underline{a}$, $\phi_c = \arccos(a/L)$,

$$C_5 = (1/2)[b\cos(\phi_c) - a\sin(\phi_c)][\cos^2(\phi_c)/a\sin(\phi_c)]$$

$$= (a^2/2L^2)[b/(L^2 - a^2)^{1/2} - 1] \qquad (30).$$

For $\underline{L} \geq \underline{b}$, $\phi_c = \arcsin(b/L)$,

$$C_6 = (1/2)[a\sin(\phi_c) - b\cos(\phi_c)][\sin^2(\phi_c)/b\cos(\phi_c)]$$

$$= (b^2/2L^2)[a/(L^2 - b^2)^{1/2} - 1] \qquad (31).$$

From these six relationships, it follows that the frequency distribution of $\underline{L}$ is of the form shown in Fig. 10 and described in normalized form by Equations (32), (33), and (34).

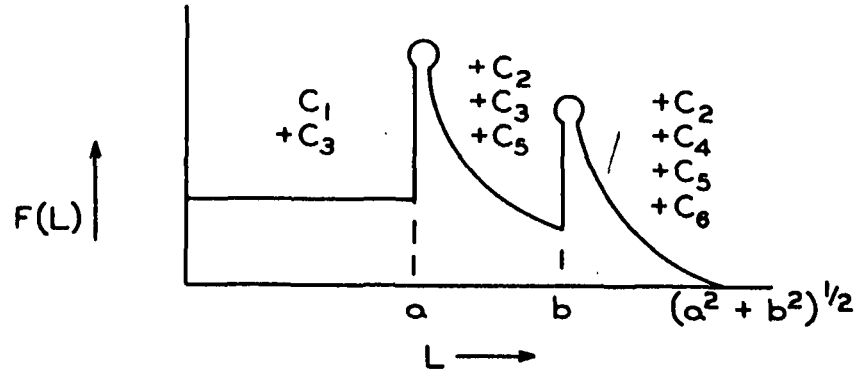

Figure 10. Frequency Distribution of $\underline{L}$, Rectangular Grid

For $0 \leq \underline{L} \leq \underline{a}$,

$$F(L) = 1/(a + b) \qquad (32).$$

For $\underline{a} \leq \underline{L} \leq \underline{b}$,

$$F(L) = a^2b/[(a + b)L^2(L^2 - a^2)^{1/2}] \qquad (33).$$

For $\underline{b} \leq \underline{L} \leq (a^2 + b^2)^{1/2}$,

$$F(L) = a^2b/[(a + b)L^2(L^2 - a^2)^{1/2}] + ab^2/[(a + b)L^2(L^2 - b^2)^{1/2}] - 1/(a + b) \quad (34).$$

Using these expressions for the distribution of $\underline{L}$, the average retention probability can be determined from Equation (23) provided the constant $\underline{B}_{\underline{L}}$ can be evaluated. From the basic properties of the various distribution functions, it follows that the frequency distribution of λ_1 is related to $\underline{F}(\underline{L})$ and $\underline{F}(\lambda_1|\underline{L})$ by

$$F(\lambda_1) = \int_{\lambda_1}^{\infty} F(L)F(\lambda_1|L)dL \quad (35).$$

Combining this expression with Equation (22) gives

$$F(\lambda_1) = B_L \int_{\lambda_1}^{\infty} F(L)dL \quad (36).$$

$\underline{F}(\lambda_1)$ can be determined, therefore, by substituting the expressions for $\underline{F}(\underline{L})$ from Equations (32), (33), and (34) into Equation (36) and integrating. Normalization of the resulting expression for $\underline{F}(\lambda_1)$ shows that the constant $\underline{B}_{\underline{L}}$ is equal to $1/\overline{\underline{L}}$ where $\overline{\underline{L}}$ is given by

$$\overline{L} = \int_0^{\infty} LF(L)dL / \int_0^{\infty} F(L)dL = \int_0^{\infty} LF(L)dL \quad (37).$$

For a rectangular-mesh network, this reduces to

$$\overline{L}_o = \pi ab/[2(a + b)] \quad (38).$$

It is interesting to note the similarity between this average network dimension and the equivalent dimension used by Estridge in his discussion of the efficiency of idealized filtration or screening operations. The dimension he employed is

equal to $\underline{ab}/(\underline{a} + \underline{b})$. Both of these dimensions might be considered as modified hydraulic radii.

The rate of initial retention can now be determined by combining Equations (5), (23), (32), (33), (34), and (38). By numerically integrating Equation (23), values of the initial retention probability have been determined for rectangular grids having side ratios of 1, 2, and 5. These values are given in Table II where $\underline{a}/\underline{L_f}$ and $\overline{L}_o/\underline{L_f}$ are both given as parameters. The agreement is extremely good between these values and those determined by the Monte-Carlo experiments.

NATURE OF THE MODEL FOR RANDOM NETWORKS

As far as present interest in the process of fiber retention is concerned, the existence of a random network is purely hypothetical. Formation of a random fiber network by deposition from a suspension of randomly distributed fibers would require complete retention. Even then, the presence of the original grid, unless it were also of random construction, would impart a degree of nonrandomness to the combined network. Retention by a random network is considered here solely for the purpose of comparison.

A random fiber network is here defined as one in which the distribution of fiber centers is random and of uniform density over the area of the network, and the distribution of angular orientations of the fibers in the plane of the network is random and of uniform density over the total angle 2π. The nature of similar networks has been treated rather extensively by Van den Akker (8) and by Kallmes and Corte (2).

To pass a scan line across a random network and note the points of intersection of the line with members of the network is equivalent to placing points

TABLE II

PROBABILITY OF INITIAL FIBER RETENTION BY A RECTANGULAR GRID—
VALUES DETERMINED USING THE NETWORK MODEL

b/a = 1			b/a = 2			b/a = 5		
$\bar{L}/L_f$	a/L_f	$\bar{R}_o$	$\bar{L}/L_f$	a/L_f	$\bar{R}_o$	$\bar{L}/L_f$	a/L_f	$\bar{R}_o$
	0.1	0.994						
0.1		0.990	0.1		0.988	0.1		0.980
	0.2	0.974		0.1	0.987		0.1	0.963
0.2		0.957	0.2		0.950	0.2		0.877
	0.3	0.939		0.2	0.945		0.2	0.807
0.3		0.894	0.3		0.840	0.3		0.769
	0.4	0.880		0.3	0.816		0.3	0.675
	0.5	0.743	0.4		0.674	0.4		0.667
0.4		0.720		0.4	0.643	0.5		0.562
	0.6	0.529	0.5		0.509		0.4	0.536
0.5		0.463		0.5	0.468	0.6		0.450
	0.7	0.365	0.6		0.345		0.5	0.382
0.6		0.284		0.6	0.307	0.7		0.321
	0.8	0.246	0.7		0.228		0.6	0.229
0.7		0.172		0.7	0.198	0.8		0.216
	0.9	0.167	0.8		0.149	0.9		0.141
	1.0	0.125		0.8	0.127		0.7	0.131
0.8		0.120	0.9		0.099	1.0		0.090
	1.1	0.103		0.9	0.084		0.8	0.715
0.9		0.095	1.0		0.070	1.1		0.055
	1.2	0.087		1.0	0.062		0.9	0.038
1.0		0.077	1.1		0.057	1.2		0.035
	1.3	0.074		1.1	0.052	1.3		0.025
	1.4	0.064	1.2		0.048		1.0	0.025
1.1		0.064		1.2	0.043	1.4		0.022
1.2		0.054	1.3		0.041		1.1	0.021
1.3		0.046		1.3	0.037	1.5		0.019
1.4		0.039	1.4		0.035		1.2	0.017
				1.4	0.032			

at random positions along the line (2). The frequency distribution of the distances between such points is of a negative exponential form. Since these distances are identical with the distance $\underline{L}$, it follows that the frequency distribution of $\underline{L}$ for a random network is given by

$$F(L) = (1/\overline{L}) \exp(-L/\overline{L}) \qquad (39),$$

where $\overline{L}$ is the average value of $\underline{L}$ as defined by Equation (37). The conditional distribution $\underline{F}(\lambda_1 | \underline{L})$ can again be shown to be equal to $1/\overline{L}$ by solving Equation (36) for $\underline{F}(\lambda_1)$ and normalizing the result. The average retention probability can now be determined by substituting Equation (39) into Equation (23) and integrating. Values of the average retention probability for a random network, as determined by numerical integration of Equation (23), are given in Table III.

TABLE III

PROBABILITY OF FIBER RETENTION BY A RANDOM NETWORK

$\overline{L}/L_f$	$\overline{P}_i$
0.01	0.999
0.05	0.990
0.10	0.948
0.20	0.762
0.30	0.574
0.40	0.434
0.50	0.336
0.60	0.266
0.70	0.215
0.80	0.177
0.90	0.148
1.00	0.126
1.10	0.108
1.20	0.094
1.30	0.082
1.40	0.073

Fiber retention by random networks is compared with fiber retention by rectangular-mesh networks in Fig. 11 where the average retention probability is shown as a function of the ratio $\bar{L}/L_f$. The relative placement of the curves corresponds to what would be predicted from a comparison of the different distributions of L. The L distribution for a random network covers a much broader range than the L distribution for a rectangular-mesh network of the same average value. It would be expected that the low-frequency spread toward high values of L would allow more fibers to escape retention by a random network when the $\bar{L}/L_f$ ratio is small. Conversely, the low frequency of low values of L should allow more fibers to escape retention by a rectangular-mesh network when the $\bar{L}/L_f$ ratio is large. The curves of Fig. 11 support this concept.

A network is random as defined above if the distributions of fiber centers and angular orientations are random and of uniform densities. The fiber-wire networks formed by the retention of fibers on rectangular grids deviate from randomness in both these respects in addition to the marked deviation of the grid itself. For high rates of initial retention, the retained fibers should form a network that closely approximates a random network. The higher the initial retention rate, however, the more appreciable is the effect of the presence of the grid upon the distribution of L at a given rate of retention.

NATURE OF THE MODEL FOR NETWORKS IN GENERAL

In order to use the Network Model to describe the change in the average retention probability with the amount of retained fibers, it is necessary to know how the distribution of L changes with retention. For a network consisting of a rectangular grid and a few retained fibers, it would not be impossible to determine the nature of the L distribution by an analysis similar to that used

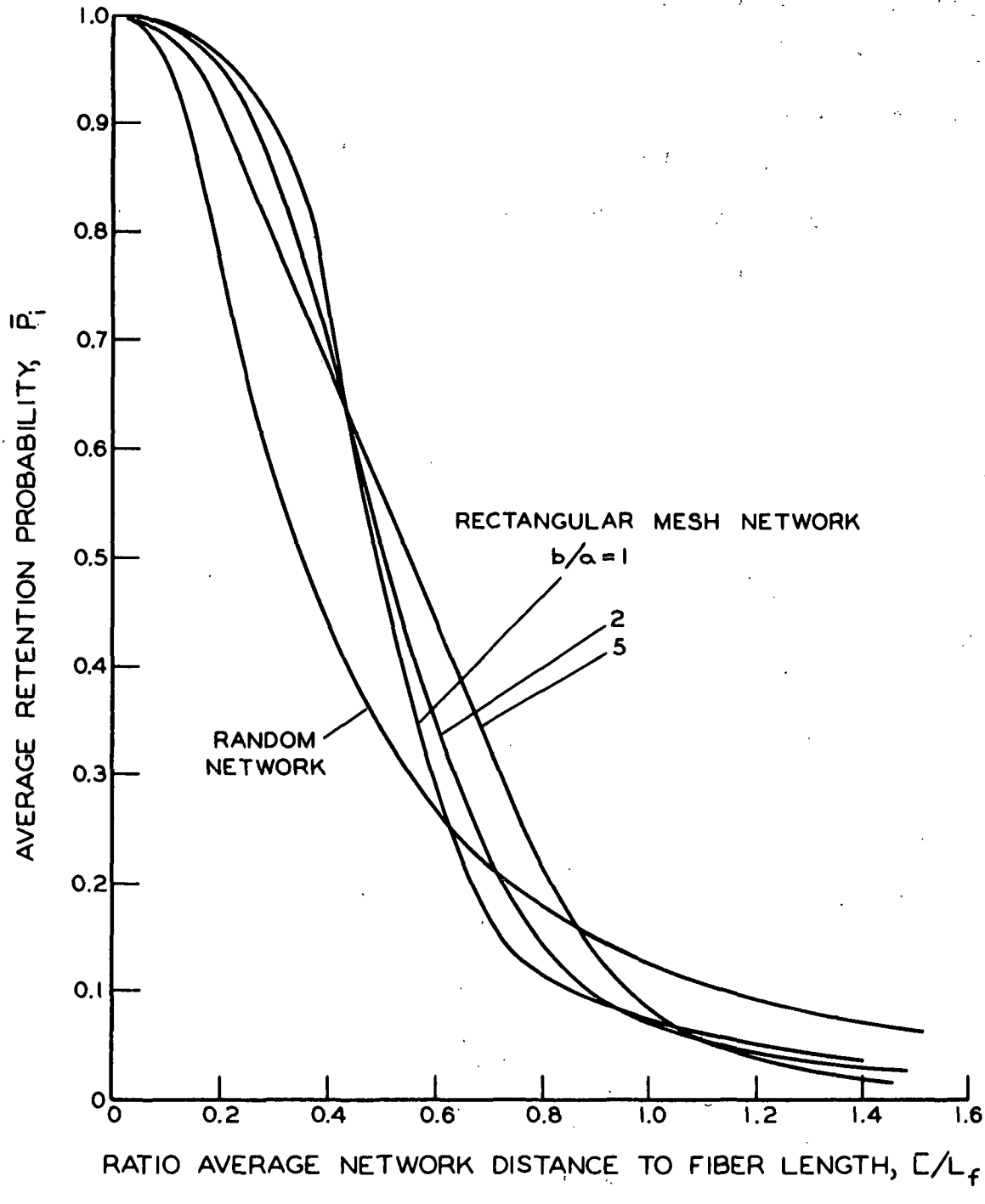

Figure 11. Average Retention Probability for Rectangular-Mesh and Random Networks

for the rectangular-mesh networks. The limitation to using this approach, however, is again the necessity of having an explicit description of the network geometry. One way of circumventing this limitation is to determine the nature of the $\underline{L}$ distribution by empirical analysis. As mentioned in the preceding section, the distances along a scan line between intersections with members of the network are identical with values of the distance $\underline{L}$. For a particular network, therefore, the distribution of $\underline{L}$ can be determined by actual physical measurement. One objective of the experimental phase of this study has been to demonstrate that the distribution of $\underline{L}$ can be determined physically in this manner.

Not knowing the exact nature of the $\underline{L}$ distribution for a general fiber-wire network, it is impossible to check the empirical distributions. It is possible, however, to check the average value of $\underline{L}$ as defined by Equation (37). From the scan-line relationship stemming from Buffon's Needle Problem, it can be shown that*

$$\bar{L} = (\pi/2)[1/(\zeta_o + \zeta_f)] \qquad (40),$$

where ζ_o and ζ_f are, respectively, the length of grid and the length of fiber per unit area. These, in turn, are

$$\zeta_o = (a + b)/ab \qquad (41)$$

and

$$\zeta_f = W_r/Aw \qquad (42),$$

where $\underline{w}$ is the mass of fiber per unit length. These relationships permit a check of the measured value of $\bar{L}$ against known network properties.

*See Appendix I, page 88.

THE EMPIRICAL METHOD OF SINGLE DIMENSION

The empirical determination of the frequency distribution of $\underline{L}$ makes it possible to apply the Network Model to predict the average retention probability for any fiber-network combination, provided the restricting conditions are observed. Eventually, an empirical description of the manner in which the distribution of $\underline{L}$ changes with retention should eliminate the need for physical measurement. Since it is already possible to calculate the average value of $\underline{L}$ from Equation (40), however, it would be extremely useful to be able to correlate the fiber retention process on the basis of this single dimension.

Consider again the hypothetical case of fiber retention by a random network. If it is assumed that the network remains random throughout the retention process, then a plot of the rate of retention versus the ratio $\overline{L}/\underline{L_f}$ will be the same as the curve of Fig. 11. Except for large values of $\overline{L}/\underline{L_f}$, this retention curve can be described by

$$R = dW_r/dW_t = 1 - B \exp(-HL_f/\overline{L}) \qquad (43),$$

where $\underline{H}$ and $\underline{B}$ are constants and the value of $\underline{H}$ is 0.31. If this equation is combined with Equation (40), it can be shown that

$$W_t = W_r + (1/K) \ln \left\{[1 - (1 - R_o) \exp(-KW_r)]/R_o\right\} \qquad (44),$$

where $\underline{R_o}$ is the rate of initial retention and $\underline{K}$ is given by

$$K = (2L_f/\pi w)H \qquad (45).$$

Estridge has already suggested that it might be possible to describe the retention process by the relationship of Equation (44) and has further shown how this relationship is dependent upon a single fictitious dimension characteristic of

the retaining network. The dimension assumed by Estridge is nonlinearly related to $\bar{L}$. By transformation of Equation (44), it can be shown that a semilogarithmic plot of white water consistency versus the mass of retained fibers should be linear. Using this type of plot, Han (22) has demonstrated that the equation is applicable to the treatment of fiber retention data in pulp systems.

In order to establish the fiber retention curve from Equation (44), it is necessary to know the value of the empirical constant K. Equation (45) shows the value of K to be dependent upon the fiber length, the mass per unit length of fiber, and the value of the constant H. By taking the second derivative of R with respect to $\bar{L}$ in Equation (43), it can be shown that the point of inflection in the R-versus-$\bar{L}/L_f$ curve occurs at a value of $\bar{L}/L_f$ equal to $H/2$. This, however, gives no real indication of how H depends upon the fundamental variables of the system. It is reasonable to expect that H is in some way dependent upon the size and shape of the initial grid openings and the relative fiber dimensions. The curves of Fig. 11 leave little doubt as to the influence of the relative dimensions of the original grid openings, the initial retention probability for a given $\bar{L}_o/L_f$ ratio being strongly dependent upon the grid structure. Dimensionally, H should be a function of the initial length ratio and the initial retention probability. It would be expected, however, that its value should be close to that determined for the random network system. If it is found that Equation (44) describes specific retention processes using a predictable value of K, then it can be used to predict retention in other systems.

From Equation (44), it can be shown that

$$K = (1/W_p) \ln (1/R_o) \qquad (46),$$

where W_p is the total mass of fibers passed unretained throughout the entire fiber retention process. Referring again to Fig. 1, W_p is equal to the value of W_t determined by extending the unit slope portion of the retention curve to $W_r = 0$. The value of the constant K can thus be determined directly from the known rate of initial retention and the measured mass of unretained fibers, provided the process is carried to the region of complete retention.

EXPERIMENTAL

OBJECTIVES AND GENERAL DESIGN OF THE RETENTION EXPERIMENTS

The Network Model provides a method of describing the process of fiber retention which does not require an explicit description of the geometry of the retaining network. The validity of the model has already been demonstrated by using it to predict previously verified values of the initial retention probability. Successful application of the network model in predicting the retention probability beyond the stage of initial retention is dependent upon two main factors. First, it must be demonstrated that the measured distribution of $\underline{L}$ adequately represents the actual distribution of $\underline{L}$. As discussed above, it is possible to compare the actual and measured distributions in terms of their average values. The second factor upon which successful application of the model depends is the extent to which the physical system meets the limitations imposed in the development of the correlation. These limitations are observed, insofar as possible, in the design of the experiments.

In addition to determining the applicability of the network model, an objective of the experimental portion of this work has been to determine whether the fiber retention process can be adequately correlated by the empirical method of single dimension. The data required to accomplish these objectives includes mass data from which retention curves similar to the one of Fig. 1 can be established, and length data from which the distributions of network distances can be established.

The retention experiments were designed so as to duplicate as well as possible the restricting conditions set forth in the development of the correlation methods. Nylon fibers were used in order to satisfy the condition that the

fibers be straight and rigid as well as to permit the study of systems containing essentially a single fiber length. To satisfy the condition that the approaching fibers be randomly distributed with respect to position and orientation, the apparatus was designed so that the approaching flow would be turbulent and so that the approaching suspension would be sufficiently dilute that fiber-fiber interaction could be neglected. For the most part, the suspension-network interactions are inherent in the retention process and cannot be completely eliminated. The extent to which these interactions affect the process is discussed in a later section.

The manner in which the required data were obtained can be explained as follows. The mass of approaching fibers was determined from the consistency and flow rate of the feed. The mass of successive increments of unretained fibers was measured and the mass of retained fibers then determined by difference. This permitted an entire retention curve to be established from each experimental run. To obtain the length data, a photograph was taken of the fiber-wire network existing at the time each sample of unretained fibers was taken. The distance distributions were then established by placing random scan lines on the photographs and measuring the distances between intersections with members of the network.

THE FIBER RETENTION APPARATUS

The apparatus used in this study is shown schematically in Fig. 12. The principal components of the system are the three stainless steel tanks, A, B, and C, the Lucite flow tube, D, the Lucite collecting tubes, E and F, and bronze pump, G, and the camera, H. Other components include the stirrer, I, the orifice, J, and copper and brass piping and valves. Microswitch relays connected with Valves V_1 and V_2 control the power supply to two electric timers associated with the collecting tubes, E and F. The flow tube can be filled from the bottom using water

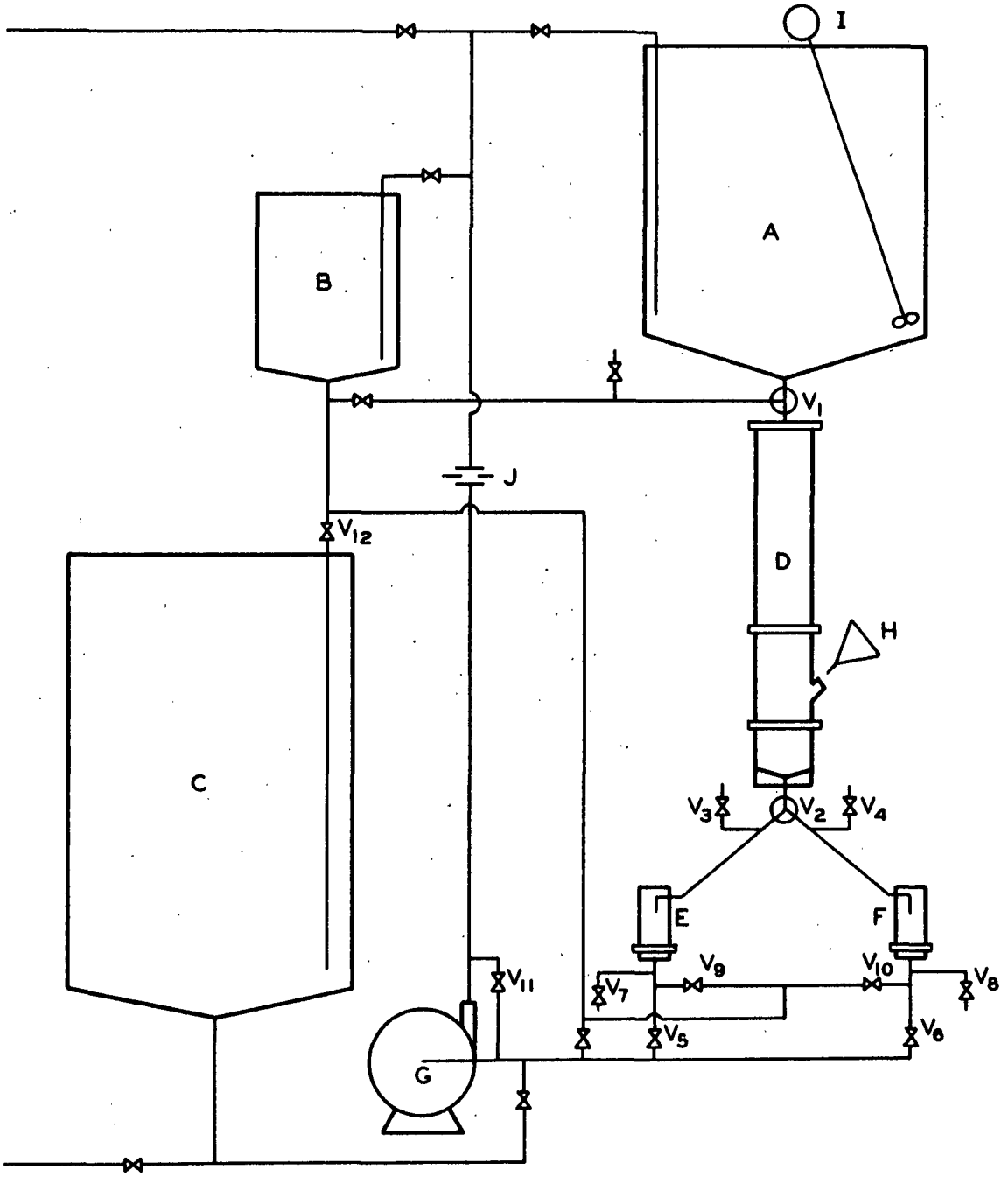

Figure 12. Schematic Representation of Fiber Retention Apparatus

from Tank B. Flow can then be established from either Tank A or B, depending on the position of Valve V_1, and the flow rate determined from the pressure drop across the orifice, J.

The main flow tube is shown in more detail in Fig. 13. The diameter is 20 cm., and the total length is 180 cm., 25 cm. of which is downstream of the retaining wire, F-F. The flow-distributing cone extends 30 cm. below the 5-cm. diameter entrance, and the longitudinal straightening vanes extend from the mid-point of the cone to within 50 cm. of the retaining wire. The turbulence-generating bank of 1.3-cm. diameter rods spaced 2.6 cm. on centers is 36 cm. above the retaining wire. The photo-window tube is 4.5 cm. in diameter and has a clear Lucite disk mounted at right angles to its axis. This tube is mounted in the side of the main flow tube such that their respective axes lie at 45 degrees to each other and intersect in the plane of the retaining wire. The camera is mounted independently of the tube.

The design of the collecting tubes is shown in more detail in Fig. 14. The inside diameter is 7.6 cm., and the flow section has a total length above the septum of 15 cm. with the straightening vanes extending to within 3 cm. of the septum. These tubes were designed so as to permit the septums to be changed easily and rapidly. The septums themselves consist of 150-mesh brass screens sealed with epoxy cement to 0.15-cm. thick brass rings and covered with sheets of tea-bag stock. There are "O"-ring seals, both top and bottom, between the septums and the tubes, and Lucite flanges to permit rapid centering. The pressure required to seal the tubes is applied by means of quick-throw clamps which press against the center of steel caps at the top of the tubes. Tygon tubing, 2.5 cm. in diameter, is used between Valve V_2 and the collecting tubes so that the top section of the tubes can be removed easily after releasing the

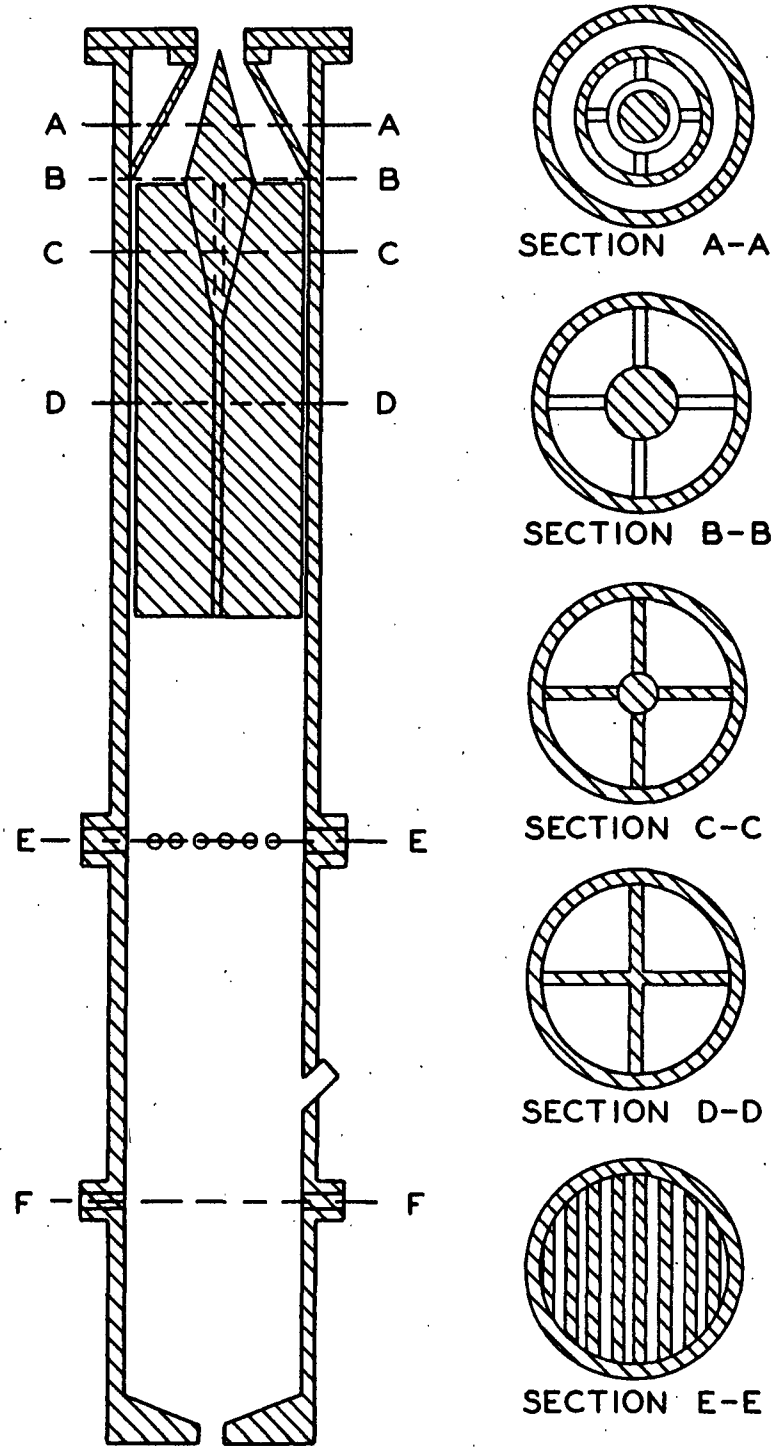

Figure 13. Main Flow Tube

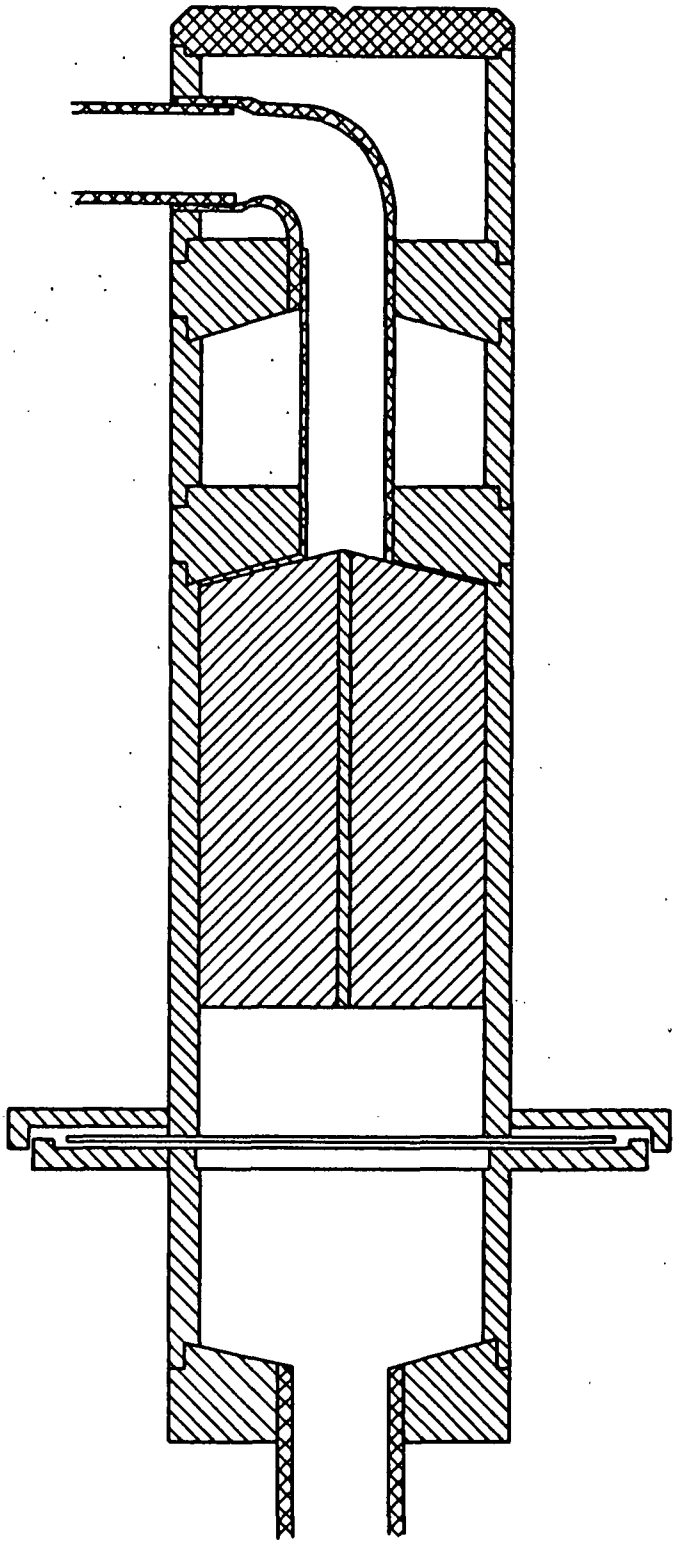

Figure 14. Collecting Tubes

clamps. Valve V_2 is a three-way plug valve which has been modified so that flow is never completely obstructed in switching from one collecting tube to the other.

FIBERS, GRIDS, AND OTHER MATERIALS

The fiber samples were prepared from continuous-filament nylon yarn, using razor blade cutters similar to those used by Estridge. The cutting procedure has been described in detail by Arnold (23). The fiber-length distributions were determined by measuring optical projections of the fibers according to the procedure outlined by Estridge. All lengths were determined from samples of water-swollen fibers. Fiber samples having average lengths of 0.15, 0.215, 0.301, 0.370, and 0.509 cm. were cut from Du Pont nylon yarn 260-20-1-Z-140, which is a color-sealed, normal-tenacity, black yarn. The water-swollen diameter of these fiber samples was found to be extremely uniform and equal to 4.1×10^{-3} cm. Another fiber sample having an average length of 0.283 cm. was cut from Du Pont nylon yarn 15-1-0-200 and dyed with Du Pont "Acetamine" black dye. The diameter of the fibers from this yarn is approximately 4.5×10^{-3} cm. The fiber-length distributions for all six samples are given in Table VII of Appendix II.

The retaining wires were constructed of 0.013-cm. diameter stainless steel wire sealed with epoxy cement to 20-cm. inside diameter, 1.3-cm. thick Lucite rings. The wire was strung across the rings using a jig having evenly spaced gage marks. The grids were constructed with the parallel wires in one direction lying in one plane and the parallel wires in the perpendicular direction lying in another plane. The retaining wires used were all rectangular mesh, and the side ratios employed were 0.127/0.127, 0.178/0.178, 0.254/0.254, 0.356/0.356, 0.356/0.178, and 0.381/0.127, all distances being expressed in centimeters.

Because of the large volumes required, it was necessary to use distilled water in order to keep the amount of undesired suspended material at a minimum. The water was prepared and deaerated in an adjoining system and brought to the run temperature of 30 $\pm$ 1°C. before being pumped to the stock tank and the small water tank. Triton X-100 surfactant was then added in the amount of 1 p.p.m. for the purpose of aiding fiber dispersion. The importance of using a surfactant is discussed below. At the end of each run, the water, which at this point was all in the lower reservoir tank, was pumped back to the adjoining system to again be deaerated by boiling.

The photographs of the retaining network were taken with a 35-mm. Leica camera, a 135-mm. lens, and the necessary extension tubes to give an image-to-object-diameter ratio of 1:1. The film used was Kodak Plus-X Pan. The lighting was found to be extremely critical in its effect upon the quality of the photographs. The best results were obtained when the network was illuminated from the side of the tube opposite the camera. A single flood lamp positioned below the level of the network was used, and a nylon curtain was wrapped around the lower portion of the tube to yield an evenly dispersed illumination. The photo-window tube design and the use of black fibers were both extremely important to the quality of the photographs.

EXPERIMENTAL PROCEDURES

PREPARATORY PROCEDURE

Having filled Tanks A and B of Fig. 12 with water as described above and having placed the retaining wire in the main flow tube, the flow system is filled from the bottom with water from Tank B while all air is vented free. With Valve

V_1 positioned such that the flow to the main flow tube is from Tank B, the desired flow rate is established by recycling to Tank B and adjusting Valve V_{11}. The weighed fiber sample, having been dispersed in 2 to 3 liters of water by running for 100 to 200 counts in the British disintegrator, is then added to the stock tank and the total volume determined from a calibrated depth gage. The fiber concentrations used in this work were of orders of magnitude below the critical concentration defined by Mason (24), ranging from 0.5 to 2.5 x 10^{-3} g. per liter. While agitating the stock suspension for from 5 to 10 minutes, Valve V_2 is positioned so that flow is through the collecting tube, E. Then having loaded the camera and checked the water temperature, the retention run is begun.

RETENTION RUN PROCEDURE

Having prepared the system as described above, the retention run is initiated by turning Valve V_1 so that the fiber suspension flows from Tank A into the main flow tube. With Valve V_2 positioned for flow through Tube E, the positioning of Valve V_1 automatically starts the electric timer associated with Tube E. Valve V_{12} is adjusted so that gravity flow to Tank C maintains the water in Tank B at a constant level. The fibers passing unretained during the first increment of the retention run are collected on the septum of Tube E. This increment is terminated and the succeeding one begun in the following manner. A photograph is taken, and after a predetermined time lag equal to the time of flow from the retaining wire to Valve V_2, Valve V_2 is positioned so that flow is to Collecting Tube F. This automatically stops one timer and starts the other. Valve V_5 is then closed, Valves V_7 and V_3 opened, and Tube E is drained. The septum is then changed, Valve V_7 closed, Valve V_9 opened, and Tube E refilled. After venting off all the air, Valves V_3 and V_9 are closed, and Valve V_5 opened. The film is advanced in the camera, and the procedure repeated for Tube F. In this manner,

it is possible to obtain several data points in a single run. After completing the run, the unretained fiber samples are air dried on the septums and then brushed into tared weighing bottles, oven dried, and weighed. The total mass of retained fibers is also determined so that the material balance can be checked.

PROCEDURE USED IN CONVERTING THE MASS DATA TO STANDARD FORM

The data as taken experimentally are not in a readily usable form. They are therefore converted to a standard form in which the mass of fibers retained per unit area is given as a function of the total mass of fibers per unit area having reached the plane of the deposit up to that point in the run.

The reference point from which all calculations are made is Valve V_2 of Fig. 12. It is for this reason that the time lag between photographing the deposit and changing Valve V_2 has been included in the run procedure. Except for the first and last data points, therefore, the total mass of fibers per unit area having reached the deposit during the time between any two data points is merely the product of the flow rate, the time of flow, and the stock consistency divided by the cross-sectional area of the tube. The mass of fibers retained per unit area is then simply the difference between this value and the mass of unretained fibers per unit area. A simple summation procedure then converts the data to the cumulative form.

The data taken at the beginning and at the end of the run, however, must be treated differently. The time of the first point must be adjusted to account for the fact that the main flow tube is still filled with pure water when the timer is started. This is done by subtracting from the recorded time the volume of the tube between Valves V_1 and V_2 divided by the volumetric flow rate.

Similarly, the flow tube is still filled with fiber suspension when the timers are stopped at the end of the run. Experimentally, these fibers are simply added to the retained fibers and no data point established. This must be taken into account whenever the measured mass of retained fibers is used.

PROCEDURE USED IN NETWORK PHOTOGRAPH ANALYSIS

The photographs taken of the fiber-wire networks existing at various stages throughout the retention process are all foreshortened in one direction because they were taken at 45 degrees to the plane of the network. In order to bring the network geometry back to its normal proportions, the photographs were projected at a 45-degree angle onto a smooth white surface and the projections then photographed. The lens system used in projection was the same as that used in taking the original photographs. Prints were then made from this second set of photographs and the network distance distributions determined from them.

To determine the distance distributions, the test area was marked by scribing a circle of diameter $\underline{D}$ on each photograph. The position of each random scan line was then determined in the following manner. Two random numbers, $\underline{T}_5$ and $\underline{T}_6$, each independently and uniformly distributed on the interval between and including 0 and 1, were selected from a table of random numbers (25). The angle of rotation from a preset axis, $\underline{\phi}_s$, and the distance of displacement from the circle diameter, $\underline{b}'$, were then determined according to the equations

$$\phi_s = 2\pi T_5 \tag{47}$$

and

$$b' = (D/2)T_6 \tag{48}.$$

Several such lines were positioned on each photograph and the distances between intersections with numbers of the network then measured.

RESULTS AND DISCUSSION

PRESENTATION AND ANALYSIS OF THE DATA IN LIGHT OF THE NETWORK MODEL

The initial length ratios and retention probabilities for the systems studied experimentally are given in Table IV. The fiber retention mass data for these systems are given in Table VIII of Appendix II. Examples of the fiber retention curves representing these data are given in Fig. 15 and 16, where the number of fibers retained per grid opening is plotted as a function of the total number of fibers per grid opening. Expressing the data in this form permits a comparison to be made between geometrically similar systems having different absolute dimensions. The curves of Fig. 15 and 16 show the reproducibility of the data to be quite good. Figure 16 shows the retention curve of Run 5 to be in disagreement with the curves of Runs 6 and 7, the retention in this run being low. The only other data showing appreciable deviation as compared with the data of other runs are those of Run 8. The retention in this run appears to be high. The data also show good agreement with the data reported by Estridge, as is illustrated in Fig. 17. The data of Run 9 fall below Estridge's data for a similar system, but the majority of the data are in good agreement. The method Estridge used to determine the rate of initial retention was to plot the ratio of the retained fiber mass to the total fiber mass as a function of the mass of retained fibers and to extrapolate to $\underline{W}_{\underline{r}} = 0$, the intercept being equal to the initial rate. The initial retention rates determined from the data of Table VIII by this method show even better agreement with the theoretical values than did the results of Estridge.

Estridge demonstrated that consistency, flow rate, and wire diameter were not significant variables in ideal systems such as those studied in this work.

That consistency and flow rate have no appreciable effect over the limited range covered is further supported by the curves of Fig. 17. The average linear velocity of the approaching suspension was 2.2 cm./sec. in Estridge's work and 3.8 cm./sec. in this work. The consistency of the approaching suspension in the runs of this work varied from 0.5×10^{-3} to 2.5×10^{-3} g./liter, which is better than a factor of 10 more dilute than the consistencies used by Estridge.

TABLE IV

INITIAL LENGTH RATIOS AND RETENTION PROBABILITIES
FOR EXPERIMENTAL FIBER RETENTION SYSTEMS

Run	$\bar{L}_o/L_f$	R_o	b/a
1	0.756	0.135	
2	0.756	0.135	
3	0.704	0.164	
4	0.704	0.164	
5	0.669	0.198	
6	0.663	0.200	
7	0.651	0.213	
8	0.549	0.362	
9	0.540	0.382	1
10	0.540	0.382	
11	0.493	0.477	
12	0.464	0.544	
13	0.464	0.544	
14	0.464	0.544	
15	0.392	0.737	
16	0.352	0.816	
17	0.331	0.852	
18	0.619	0.372	
19	0.504	0.498	2
20	0.366	0.736	
21	0.497	0.540	
22	0.405	0.660	3
23	0.294	0.806	

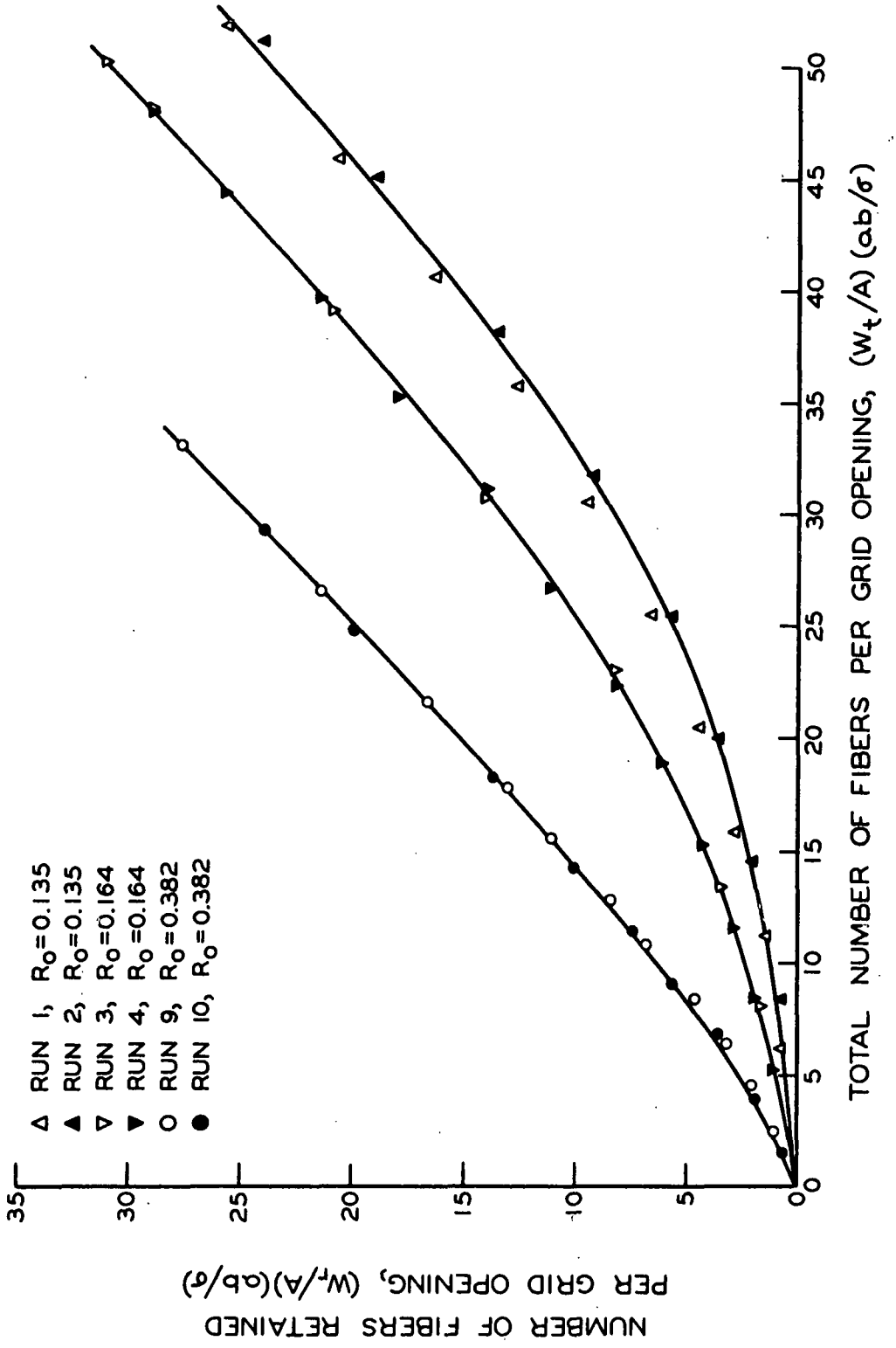

Figure 15. Experimental Fiber Retention Curves

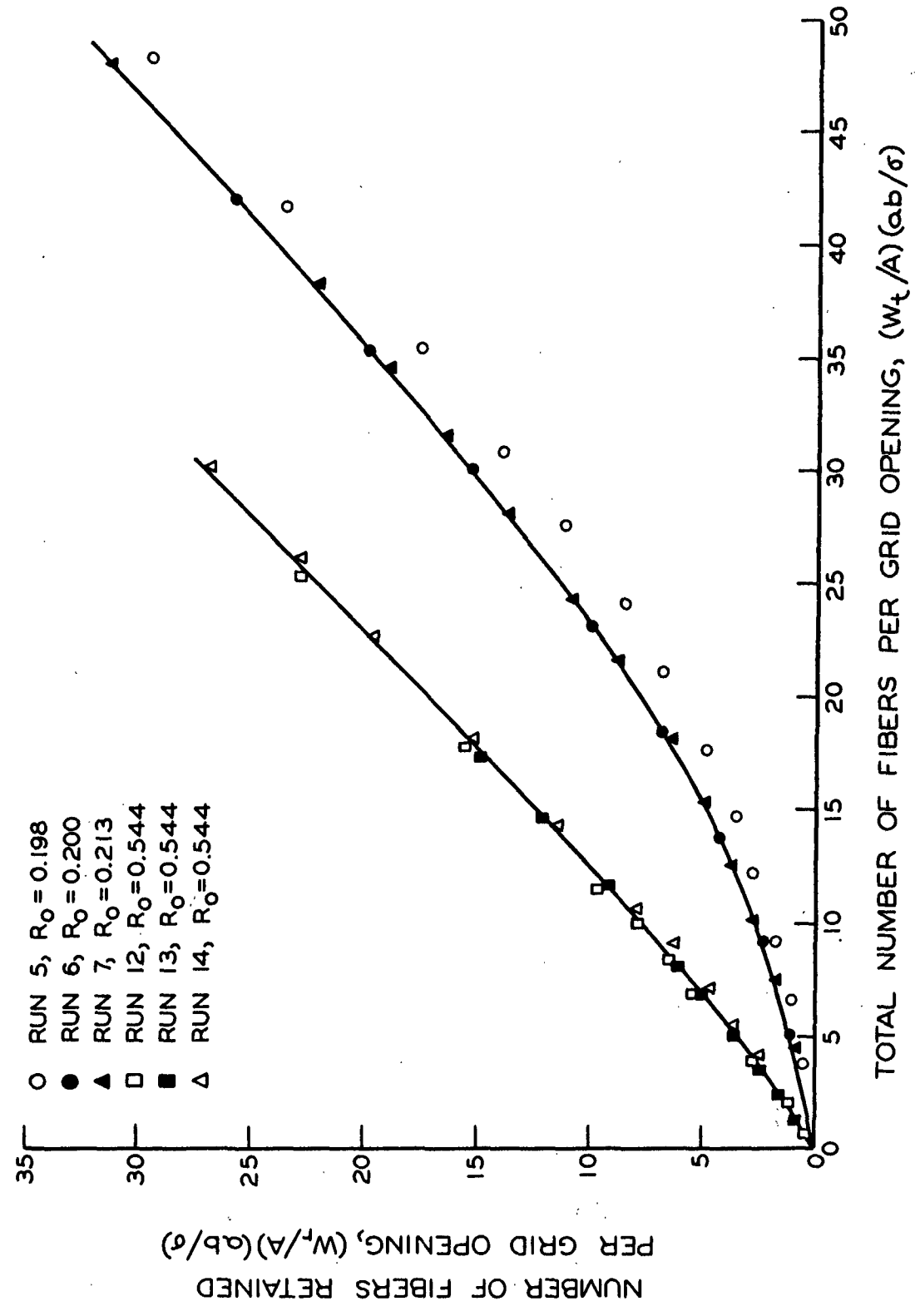

Figure 16. Experimental Fiber Retention Curves

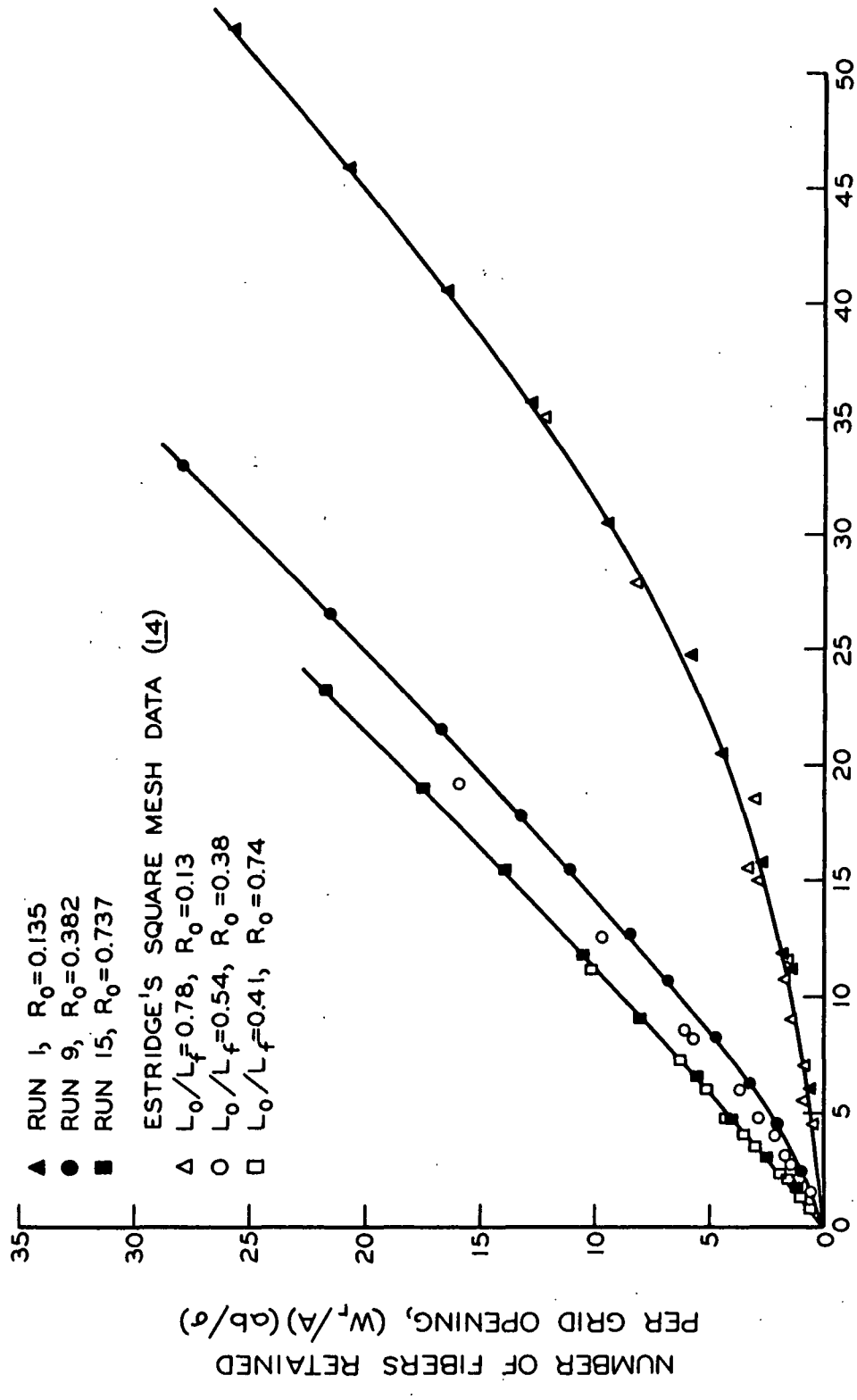

Figure 17. Comparison of Experimental Fiber Retention Curves With Those of Estridge

The data of this work indicate some slight but not significant effect of the initial length ratio. This is illustrated in Fig. 18, where fiber retention data are plotted for rectangular grids of Side Ratios 1 and 2. Runs 10 and 18, having initial retention probabilities of 0.38 and 0.37 and side ratios of 1 and 2, respectively, show the maximum deviation observed. The data of the other runs indicate that the initial length ratio has no significant effect within the limits studied other than its direct influence upon the initial retention probability.

Photographs of the fiber-wire networks of Runs 9 and 17 are shown in Fig. 19. The areas shown are those used in the network distance determinations. Several hundred distances were measured for each photograph analyzed. The general nature of the frequency distributions obtained from the scan line measurements is illustrated by the distributions for Run 17, shown in Fig. 20. The solid and dashed curves are the frequency distributions estimated from the histograms combined with a knowledge of the nature of the distribution for the bare grid. For each network analyzed, two curves were estimated. The distribution functions were then normalized by setting the area under the curves equal to unity, and the average length ratios and retention probabilities calculated from Equations (23) and (37). The results are given in Table V. Also given in Table V are the theoretical length ratios calculated from Equation (40) and the values of the fiber retention probability determined from the mass data. The method used to determine the slopes of the experimental retention curves from the mass data is as follows. The slope at the point $\underline{W}_t = \underline{V}_t$ and $\underline{W}_r = \underline{V}_r$ was determined by plotting the ratio $(\underline{W}_r - \underline{V}_r)/(\underline{W}_t - \underline{V}_t)$ as a function of $(\underline{W}_t - \underline{V}_t)/\underline{A}$ and extrapolating to $(\underline{W}_t - \underline{V}_t)/\underline{A} = 0$. The intercept at this point is equal to the slope of the fiber retention curve at the point $\underline{W}_t = \underline{V}_t$. Plots of this type are illustrated in

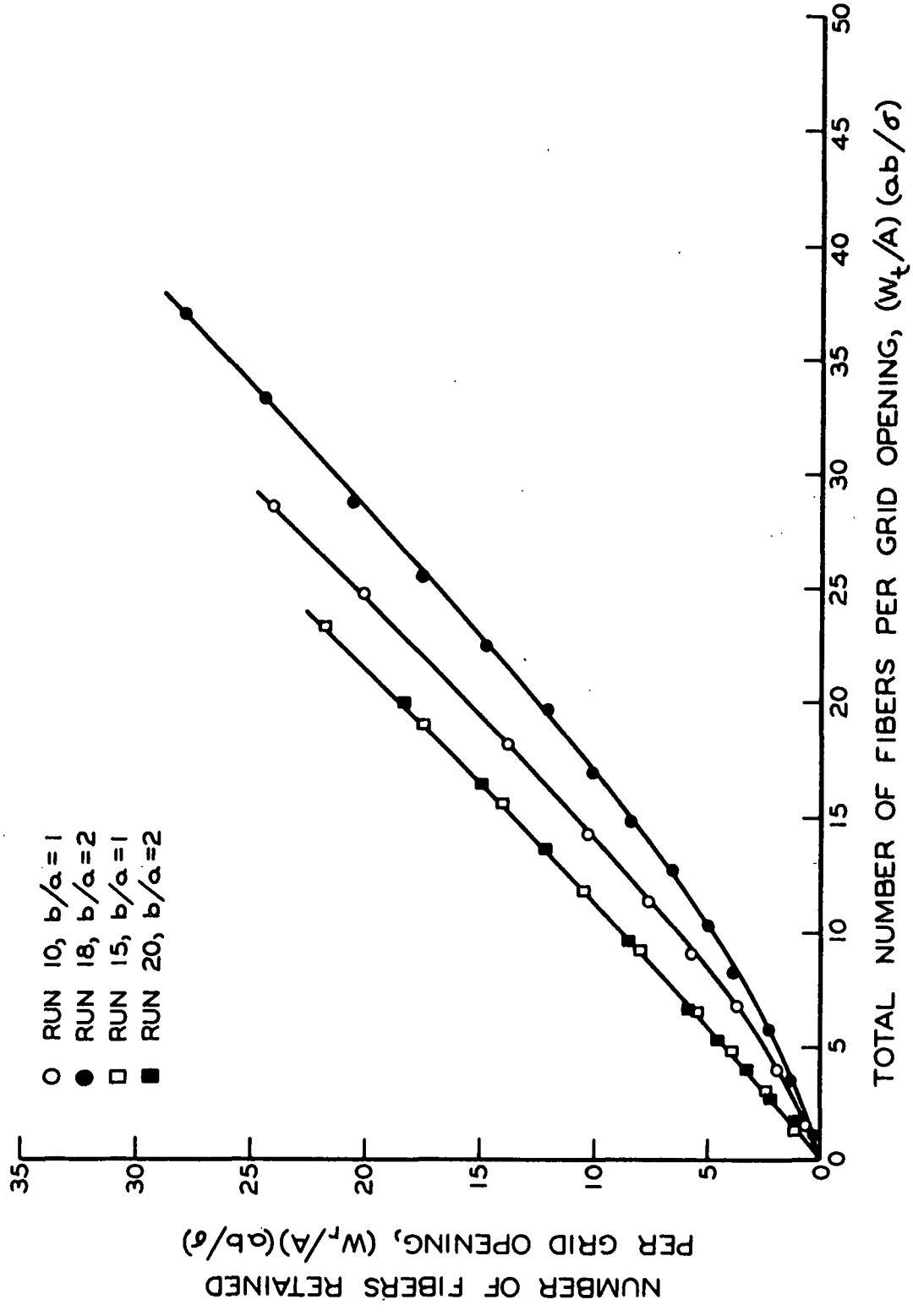

Figure 18. Comparison of Experimental Fiber Retention Curves for Systems Having Rectangular Grids of Different Side Ratios

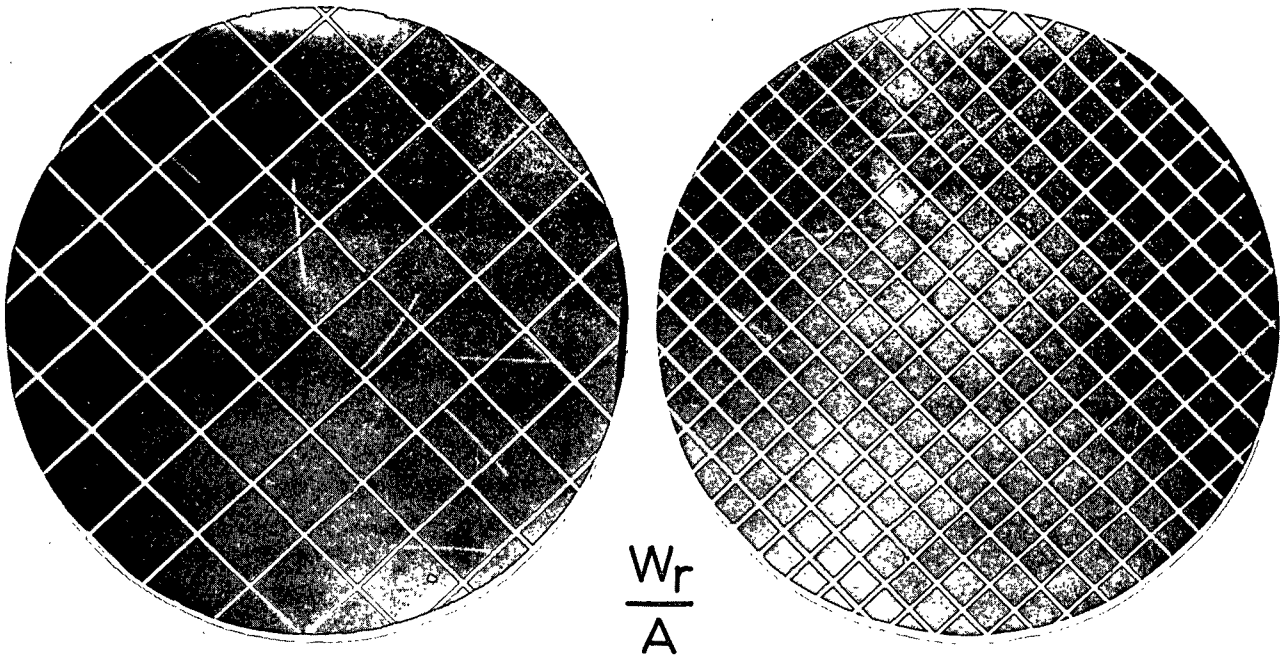

$\frac{W_r}{A}$

0.1×10^{-4} G./CM.^{2} 0 G./CM.^{2}

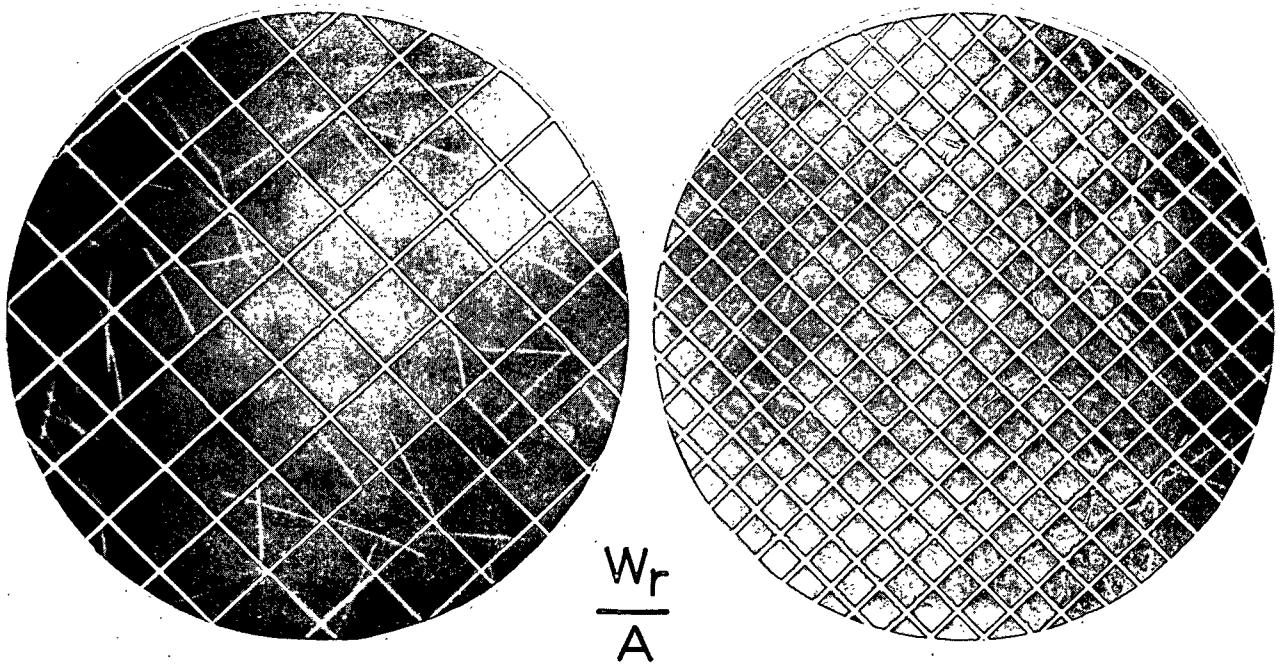

$\frac{W_r}{A}$

0.9×10^{-4} G./CM.^{2} 1.1×10^{-4} G./CM.^{2}

$a = 0.254$ CM. $a = 0.127$ CM.

$L_f = 0.370$ CM. $L_f = 0.301$ CM.

Figure 19a. Photographs of Fiber-Wire Networks, Runs 9 and 17

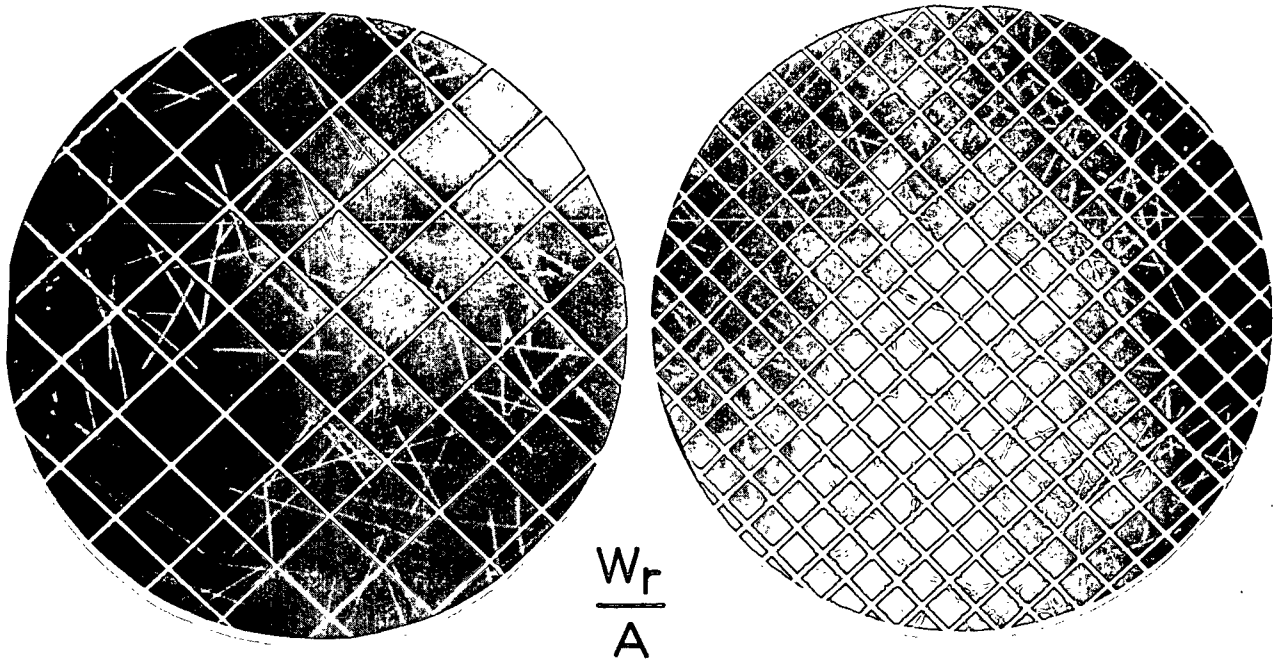

$\frac{W_r}{A}$

1.9×10^{-4} G./CM.^{2} 2.3×10^{-4} G./CM.^{2}

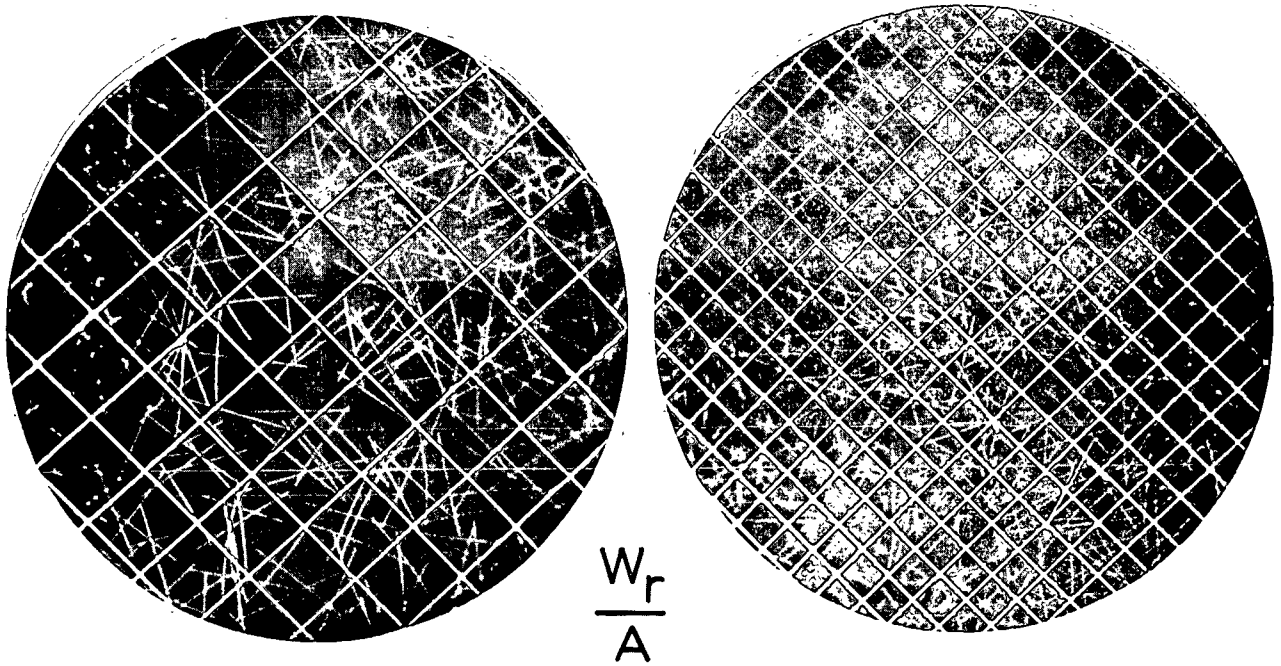

$\frac{W_r}{A}$

4.1×10^{-4} G./CM.^{2} 4.3×10^{-4} G./CM.^{2}

$a = 0.254$ CM. $a = 0.127$ CM.

$L_f = 0.370$ CM. $L_f = 0.301$ CM.

Figure 19b. Photographs of Fiber-Wire Networks, Runs 9 and 17

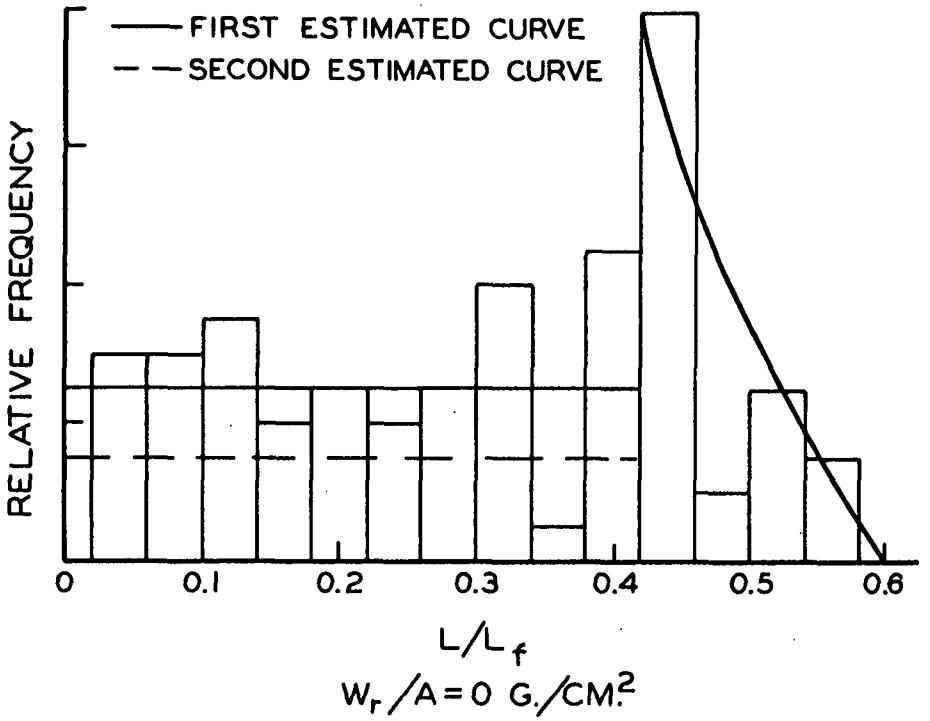

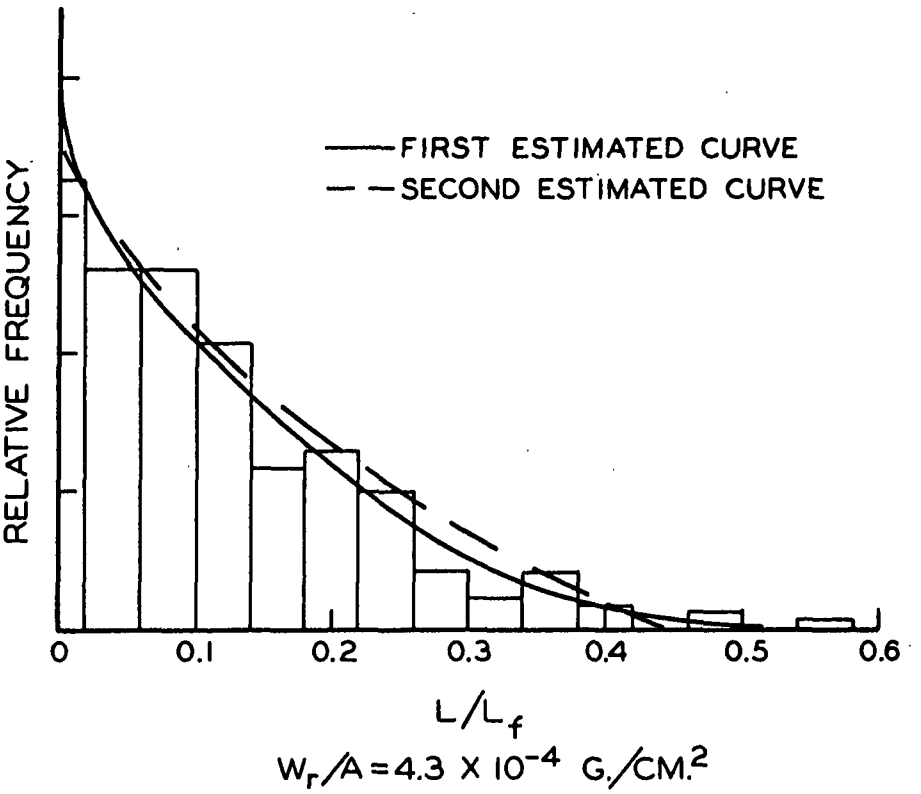

Figure 20. Network Distance Distributions Determined from Photographs, Run 17

TABLE V

VALUES OF THE AVERAGE LENGTH RATIO AND THE RETENTION PROBABILITY AS A FUNCTION OF THE MASS OF FIBERS RETAINED

Run	$(\underline{W}_r/\underline{A})\times10^4$, g./cm.^{2}	$\bar{L}/L_f$[a] A	B	C	$\underline{R}$[b] A	B	C
2	0.0	0.73	0.68	0.76	0.07	0.11	0.10
	0.3	0.55	0.46	0.48	0.13	0.31	0.33
	0.8	0.38	0.33	0.34	0.25	0.39	0.42
	1.6	0.27	0.31	0.23	0.36	0.43	0.54
	2.6	0.19	0.19	0.19	0.48	0.91	0.91
6	0.7	0.42	0.36	0.49	0.25	0.45	0.32
	1.6	0.28	0.32	0.29	0.38	0.58	0.56
	3.1	0.18	0.20	0.16	0.48	0.76	0.80
	4.8	0.13	0.16	0.15	0.60	0.91	0.92
	7.0	0.10	0.13	0.11	0.73	0.95	0.95
9	0.1	0.51	0.48	0.51	0.39	0.47	0.44
	0.9	0.31	0.50	0.33	0.49	0.60	0.65
	1.9	0.21	0.24	0.21	0.60	0.76	0.79
	4.1	0.12	0.15	0.14	0.80	0.93	0.95
12	0.5	0.36	0.29	0.33	0.59	0.64	0.62
	1.9	0.22	0.22	0.22	0.73	0.88	0.88
	3.9	0.14	0.15	0.14	0.81	0.94	0.95
17	0.0	0.33	0.33	0.35	0.86	0.94	0.92
	1.1	0.23	0.27	0.26	0.87	0.98	0.98
	2.3	0.17	0.18	0.15	0.87	0.93	0.95
	3.3	0.14	0.14	0.14	0.88	0.96	0.95
	4.3	0.12	0.14	0.13	0.89	0.95	0.95
19	0.2	0.44	0.48	0.47	0.63	0.61	0.57
	1.1	0.27	0.32	0.29	0.68	0.68	0.70
	2.0	0.19	0.22	0.20	0.73	0.80	0.83
	3.0	0.15	0.20	0.16	0.76	0.91	0.93
	4.2	0.12	0.13	0.13	0.80	0.95	0.95
20	0.3	0.30	0.27	0.29	0.78	0.81	0.79
	1.4	0.17	0.18	0.16	0.83	0.87	0.90
	2.7	0.12	0.13	0.11	0.86	0.95	0.95
	3.9	0.09	0.08	0.09	0.89	0.96	0.97
23	0.3	0.24	0.21	0.25	0.82	1.00	1.00
	1.2	0.17	0.16	0.16	0.86	1.00	1.00
	2.3	0.12	0.11	0.10	0.89	0.97	0.97
	3.2	0.10	0.11	0.10	0.91	0.97	0.97
	4.1	0.08	0.09	0.09	0.93	0.97	0.96

[a] The values of $\bar{L}/L_f$ in Column A are calculated from Equation (40), those in Columns B and C are from the first and second estimated distribution curves calculated according to Equation (37).

[b] The values of $\underline{R}$ in Column A are from the mass data, those in Columns B and C are from the first and second estimated distribution curves calculated according to Equation (23).

Fig. 21 for Run 9. The length ratios obtained from the estimated network distributions are in reasonable agreement with the theoretical values. The retention probabilities obtained from the mass data, however, are appreciably lower than those determined from the network distributions. The retention rate is plotted as a function of the average length ratio in Fig. 22 and 23 for three runs. The curves of Fig. 22 are plotted from the mass data and the curves of Fig. 23 are plotted from the photographic data. The curves for the three runs illustrated are representative of the general results, the slopes of the experimental fiber retention curves being considerably lower than predicted from the Network Model using the length distributions determined from the photographs. Although the length distributions estimated from the photographic data are only rough approximations, there is reason to believe that they are good representations of the actual fiber-wire networks. The agreement between the theoretical and measured average length ratios is indicative of this. Also, it has been found that the shape of the estimated distribution curve can be markedly changed with little effect upon the estimated retention probability. Therefore, the discrepancy between the slopes of the fiber retention curves and the retention probabilities predicted from the Network Model must be the result of some other factor or factors.

Measurements of the approaching fiber orientations through photographic analysis, as reported by Estridge, indicated some slight deviation from randomness. He did not consider this deviation to be significant. That the deviation was not significant is supported by the agreement between his data and the data of this work. The upstream portion of the main flow tube used in this work was essentially the same as the one used by Estridge except for the addition of the bank of turbulence-generating rods. Parker (26) has shown that a rod bank of this type increases turbulence. The bank of rods and the higher flow rates were

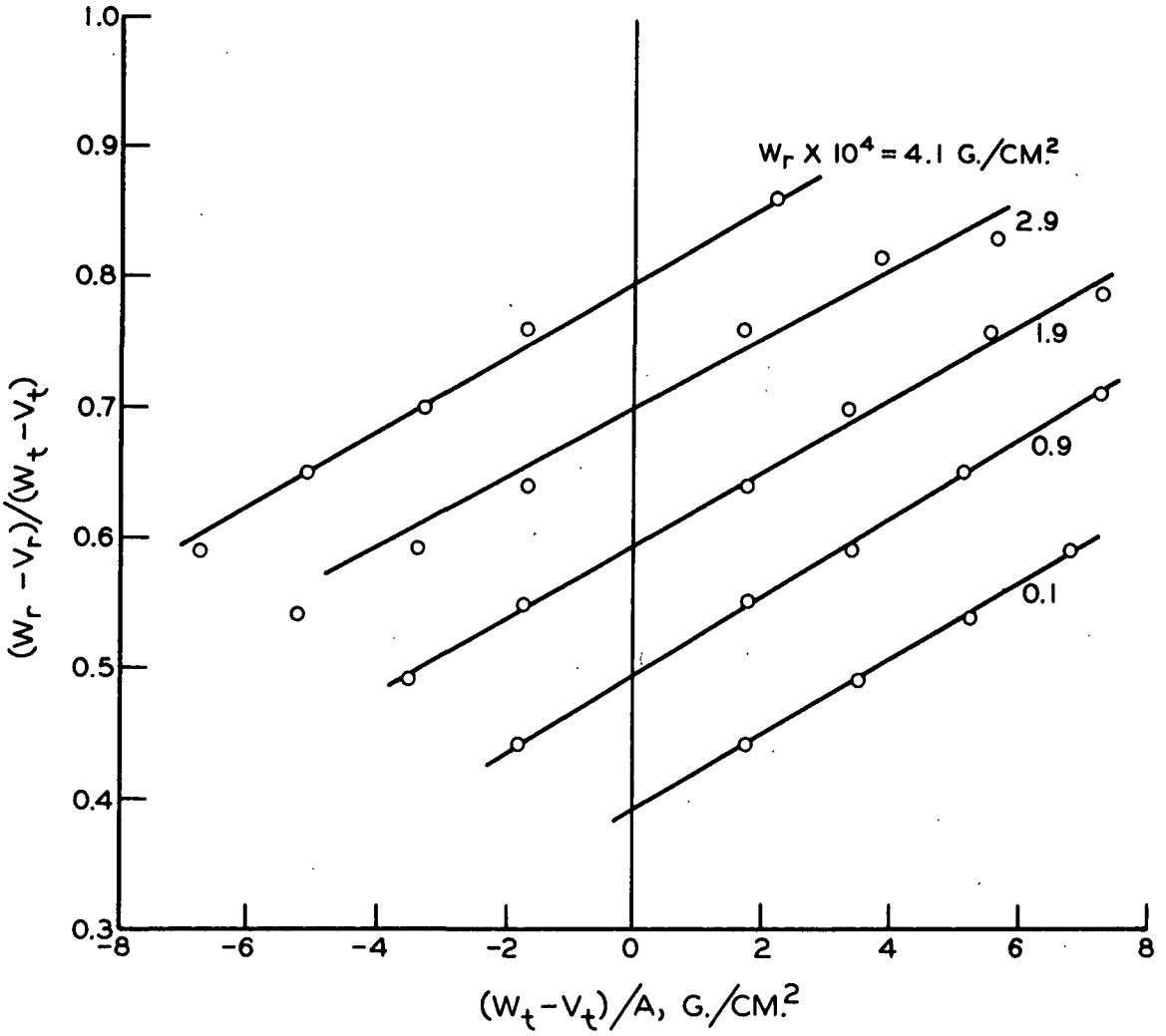

Figure 21. Determination of Average Retention Probabilities from Mass Data, Run 9

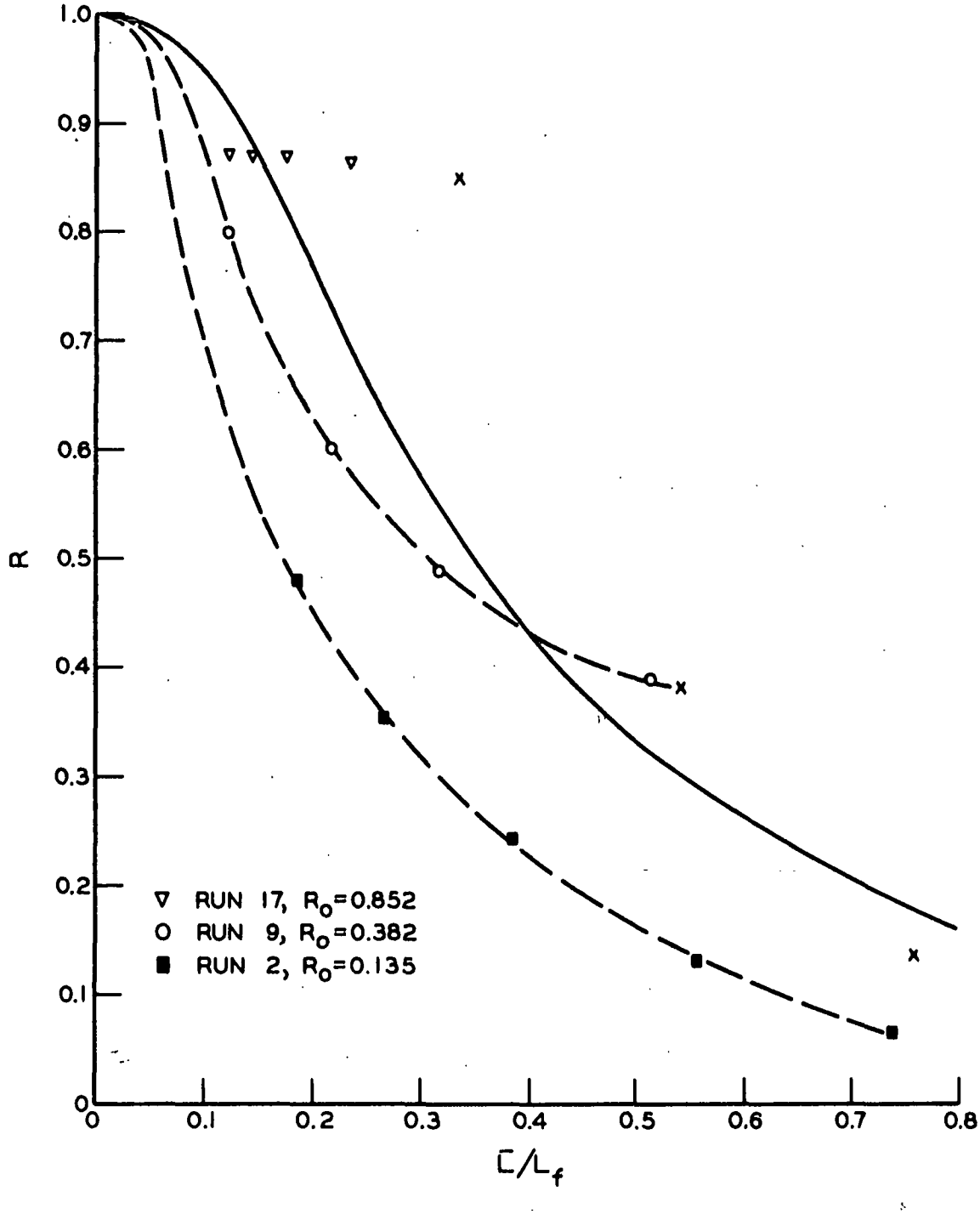

Figure 22. Average Retention Probability versus Length Ratio, Mass Data

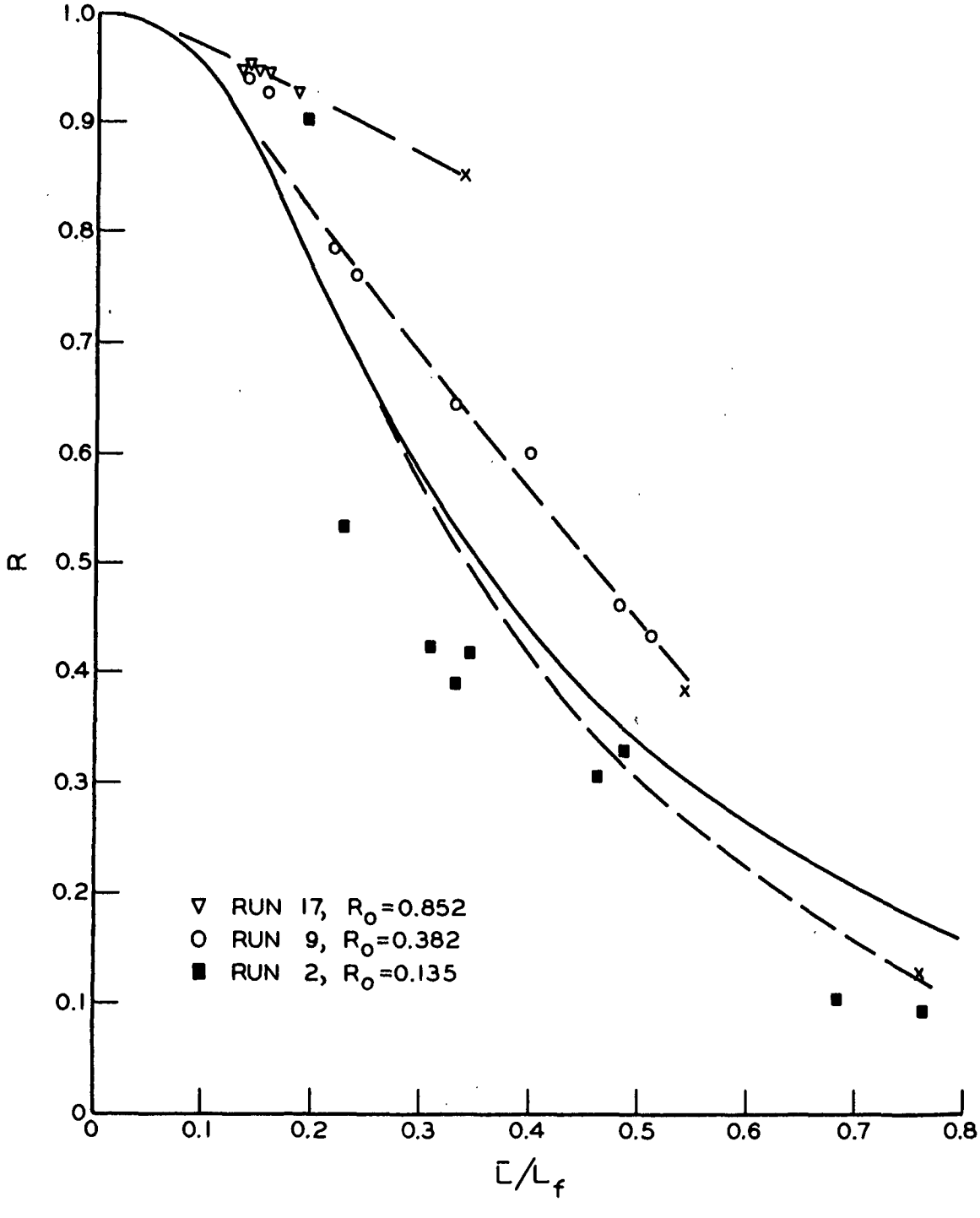

Figure 23. Average Retention Probability versus Length Ratio, Photographic Data

used in this work to insure randomness in the approaching fiber orientations. The fact that the present data agree with Estridge's gives further indication that the approaching fiber orientations were random in his system as well as in those of this work.

The difference between the measured retention rates and those predicted from the Network Model must be the result of one of two remaining factors. The discrepancy could be the result of the presence of small-scale vibrations within the system or of the presence of suspension-network interactions which were not taken into account in the application of the model. Vibrations, when present, were very definitely a problem. A few runs were made when other equipment was operating in the vicinity of the retention apparatus with the result that little if any retention occurred. Quite probably, less severe vibrations were present at all times, even though the pump was as completely isolated as possible from the rest of the apparatus. If such vibrations were great enough to affect the retention process appreciably, they would have had to be extremely uniform or the data would not have been reproducible. Again, a comparison with Estridge's system is helpful. Except for the upstream section of the main flow tube, his apparatus and the one used in this study were of completely different design. Most important, the pumps were of different design. It is quite unlikely that vibrations severe enough to affect the data would have had virtually the same effect in both systems. Therefore, the fact that the measured retention rates were lower than predicted must be attributed to the influence of suspension-network interactions.

As mentioned previously, the effects of suspension-network interactions include changes in the hydrodynamics of the suspension due to the presence of the network, changes in the network structure due to fluid drag forces, and

changes in the network structure or in the position of fibers relative to the network due to the friction and impact forces which occur as fibers come into contact with the network. Consider the possibility of the fluid drag forces appreciably changing the structure of the network. If the fibers were not sufficiently rigid, the force of fluid drag might cause bending which, if large enough, would result in the loss of some fibers from the network. The fibers used in this work, however, did not exhibit any significant amount of bending. In the case of the 0.283-cm. fibers, some slight bending did occur, as was evident from the photographs of the networks composed of these fibers. The fact that the data obtained using these fibers agree with the rest of the data shows that the degree of fiber bending was not significant. This, however, is not the only manner in which the fluid drag forces can affect the network structure. In the development of the ideal system used as a model in this work, it was assumed that upon contacting the network the depositing fibers rotate without change in the ($\underline{x}$, $\underline{y}$) co-ordinates of their centers. This would imply that the friction between the depositing fibers and the network material is so small as to be nearly negligible. The very nature of the frictional force in a system of essentially nonswelling, smooth components completely surrounded by water, would indicate that the magnitude of such a force is relatively small. The frictional force referred to here is actually a viscous drag force transmitted between the network material and the individual fiber through the intermediate liquid film. When considering whether an approaching fiber will or will not be retained it thus appears valid to assume that frictional forces are negligible. If the friction between the depositing fiber and the network material is negligible, however, then the friction between various members of the network should also be negligible. If the network were contained within a single plane, the constant downward forces of fluid drag and gravity would serve to hold all the members of the network in fixed positions. The network, however,

does not actually lie within a single plane. In fact, the grid itself does not lie in a single plane. In the absence of friction within the network, the individual members would be expected to move, under the influence of the downward forces, to positions of maximum stability. The movement within the network itself would not be expected to alter the average retention probability predicted from the Network Model because of the statistical nature of the model itself. In moving to a position of greater stability, however, the fiber may become unsupported and fall free from the network. If this happens, the result is obvious.

Next, consider the effect of the forces transmitted to the network during fiber deposition. Assume that the network is in a state of equilibrium just prior to the approach of another fiber. If the approaching fiber, upon contacting the network, exerts a large enough force on the network, the force balance will be disrupted, the consequence being similar to that discussed above. A rough comparison of the magnitudes of the fluid drag forces and the forces of fiber deposition is made in Appendix III. There is no question as to the significance of the force exerted by a fiber coming into contact with the network. In addition, the force of fiber deposition is transmitted at the single point of contact with the network. Besides losses due to general structural rearrangement as discussed above, the deposition forces may actually cause the direct loss of fibers which have been retained previously. This is particularly serious when the fiber length is shorter than the dimensions of the grid, as illustrated in Fig. 24. If the fibers in the figure are deposited in the order 1, 2, and 3, it can be seen that the first would definitely be retained, the second might be retained without forcing the first through the opening, but the third would shift the center of mass of the combined structure such that all three fibers would be lost. As shown in the figure, only the evenly distributed forces of gravity and fluid drag are considered. The situation becomes even more serious when the forces of fiber deposition are considered.

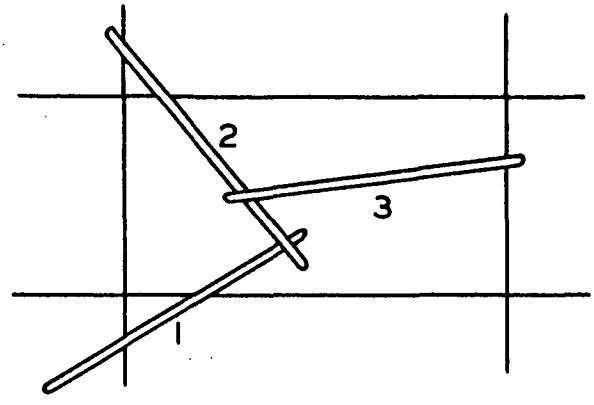

Figure 24. Example of an Unstable Network Structure

The last type of suspension-network interaction to be considered is the effect of the network structure on the hydrodynamics of the suspension. From the fundamental consideration of continuity, it is apparent that some acceleration must occur as the suspension flows into the network structure. If the linear upstream velocity is 4 cm./sec., then the superficial velocity through a network having 90% open area is nearly 4.5 cm./sec. Moss (27) has shown that fibers accelerate nearly instantaneously with the fluid. Therefore, some fiber alignment must occur in the direction of flow as the suspension enters the network. It is reasonable to assume, however, that the relatively small increases in velocity do not give rise to an appreciable degree of fiber alignment.

It is also apparent that random fiber orientation cannot exist within a distance of a fiber length of the wall of the flow tube. This was one of the reasons for using a large-diameter flow tube in this work. Andrews (28) has found that the over-all retention in a 7.5-cm. diameter tube is considerably less than the predicted initial retention. As in the systems studied in this work, several other factors were probably partially responsible for the low retention he observed.

It is reasonable to assume, however, that the magnitude of the losses he observed is directly attributable to the wall effects in the smaller diameter flow tube. The fact that the average network lengths determined from the network photographs which were taken of the center of the deposit are not consistently shorter than calculated from the mass data indicates that wall effects were not significant in this work.

One final deviation from ideality remains to be considered. In the section dealing with the conditions necessary and sufficient for retention, the possibility was discussed of a fiber being retained by a tucking-under process in which the lead end of the fiber rotates up into contact with the underside of the retaining network. This was illustrated in Fig. 4. The shorter the relative fiber length, the less this is apt to occur. At the other extreme, if the fiber is longer than twice the maximum network distance, tucking under does not increase retention since the fiber would be considered as retained in the normal manner. Although the possibility exists that some fibers which would not ordinarily be retained are retained by this mechanism, the total number of such retentions is believed to be negligible.

CORRELATION OF THE DATA USING THE METHOD OF SINGLE DIMENSION

Equation (44) has been fitted to the data of Table VIII by the method of least squares. The values of $\underline{K}$ determined in this manner are given in Table VI along with the corresponding values of $\underline{H}$. Using these values in Equation (44), the predicted values of the retained mass are within 10% of the experimental values, and for basis weights greater than 3 to 5 x 10^{-4} g./cm.^{2}, they are within 5%. Here again the fact that the retention rate predicted from the Network Model is high is reflected in the low values of $\underline{H}$ as compared with the value determined

TABLE VI

VALUES OF THE EMPIRICAL FACTORS K AND H

Run	R_o	$K \times 10^{-4}$, $cm.^2/g.$	H
1	0.135	0.16	0.10
2	0.135	0.15	0.10
3	0.164	0.11	0.11
4	0.164	0.12	0.12
5	0.198	0.06	0.10
6	0.200	0.13	0.10
7	0.213	0.08	0.09
8	0.362	0.32	0.15
9	0.382	0.22	0.14
10	0.382	0.24	0.15
11	0.477	0.17	0.17
12	0.544	0.21	0.17
13	0.544	0.19	0.15
14	0.544	0.10	0.12
15	0.737	0.18	0.09
16	0.816	0.08	0.08
17	0.852	0.09	0.07
18	0.372	0.15	0.12
19	0.498	0.23	0.15
20	0.736	0.18	0.09
21	0.540	0.17	0.13
22	0.660	0.20	0.13
23	0.806	0.17	0.08

from the random network system. As mentioned previously, the value of the constant H should be dependent upon the initial retention probability and the initial length ratio. It is not possible to determine the nature of any such dependence from the values of H given in Table VI. However, if H is taken to be a constant equal to 0.12, the predicted retention curve in most cases agrees quite well with the experimental curve. This is illustrated in Fig. 25.

Han (22) has published data for the retention of sulfite pulp using a conventional papermaking screen on a vacuum former. The consistencies employed were orders of magnitude greater than those of this work. The value of K determined from his data is 0.045×10^4 cm.^{2}/g. Although this value of K is slightly lower than the values found in the present study, the agreement is as good as might be expected. This agreement indicates that the basic nature of the retention process is no different in practical systems than it is in the ideal systems. It would be expected that retention along the nip of a single table roll would be much the same as that of the vacuum former.

EXPERIMENTAL OBSERVATIONS

In the section dealing with the preparation of the fibers, grids, and other materials, it was mentioned that a surfactant was added to the distilled water used in preparing the fiber suspensions. The method of data collection used in this study made it extremely important that the consistency of the approaching suspension remain constant with time. Ingmanson (29) had previously observed that when a fiber suspension was taken from a tank through a relatively small center drain, the consistency of the exiting suspension decreased continuously with time. He attributed this behavior to a fractionating effect at the vortex. Without proper agitation of the suspension in the tank, this is without doubt a

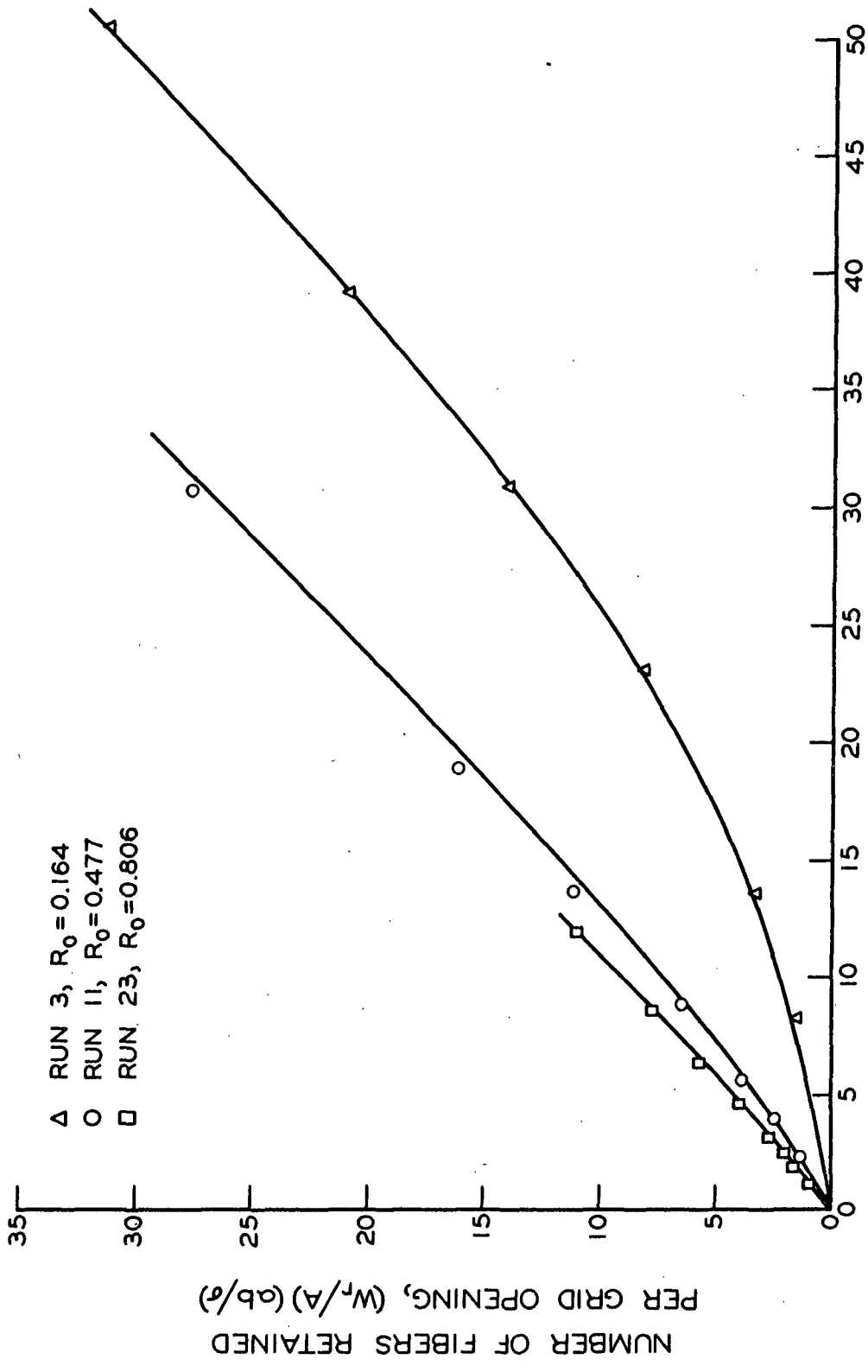

Figure 25. Fiber Retention Predicted by the Correlation Method of Single Dimension

real effect. It was observed in the work of this study, however, that as the level in the supply tank fell, a considerable number of fibers were left on the walls of the tank causing a drop in the exit consistency of up to 30%. It was then observed that if a suspension were left to agitate at constant volume, there was a build-up of fibers at the suspension-air interface. In a suspension that is being agitated, fibers are continuously coming to the surface, and it is natural to assume that fibers are also continuously leaving the surface. If the surface tension forces are sufficient to overcome the forces of agitation, however, the rate at which fibers leave the surface decreases and the fiber concentration in the surface layer increases. It has been found that the addition of a surfactant virtually eliminates any fiber concentration at the surface and any clinging of fibers to the walls of the tank. The surfactant used in this work was Triton X-100, a nonionic compound made by Rohm and Haas. A concentration of 1 p.p.m. produced the desired results.

Another observation worth mentioning concerns the efficiency of the absolute collecting septums which were used to collect the unretained fibers. The collecting tubes, as originally designed, did not have the straightening vanes, and appreciable fiber loss occurred through the 150-mesh wire screens used as septums. Theoretically a 150-mesh screen should retain nearly 100% of the fibers, but because of the flow patterns in the collecting tubes, the fibers were permitted to make multiple passes at the screens and the losses were thus multiplied. The addition of the flow-straightening vanes eliminated the fiber loss. This is a good illustration of the importance of flow conditions to the process of fiber retention.

In addition to the 35-mm. photographs which were taken of the fiber-wire networks, some 16-mm. motion pictures were taken of the fiber-retention process.

These pictures were taken to obtain a qualitative idea of the amount of movement taking place as fibers approached and contacted the network. The motion pictures were taken at 1 to 4 times normal speed. Extensive movement was observed within the networks, the order of magnitude being in the range of a fiber length. Motion pictures were taken during one run in which short fibers were used and the effects of fiber movement were exceptionally obvious. There was no net retention during this run. Fibers would be momentarily retained but would move until they fell free of the wire. The motion pictures merely served to illustrate that extensive fiber movement does occur within the fiber-wire network.

It might be mentioned that the possibility was investigated of using light-scattering techniques to monitor the downstream consistency. The apparatus used in this work was that of Johnson (13). It was impossible to detect any change in the degree of scatter with change in consistency within the range of consistencies used in the present work. It might also be mentioned that several network photographs were traced optically in a manner similar to that reported by Kallmes and Corte (2). The microdensitometer used to make these traces was that of Jentzen (30). The traces failed to record network distances which appeared shorter than the diameter of the light beam on the photographic films of the network.

APPLICATION TO SHEET FORMING IN PRACTICAL SYSTEMS

Suspension-network interactions were found to have a considerable influence upon the rates of fiber retention observed in this work. Even though the observed rates were consistently below the rates predicted from the Network Model, however, the openings of the initial grid were rapidly closed and the rate of retention approached unity at rather low basis weights. The fact that

extensive fiber losses occur during normal papermaking operations must be attributed to the presence of severe interactions, vibrations, and other influencing factors not considered in the ideal systems of this study. The basic nature of the retention process, however, remains the same.

Factors such as flocculation or general fiber-fiber interaction should serve to increase the rate of retention since the units being retained consist of several fibers and the probability of interception is greater. It is conceivable that fiber-fiber interaction might not be as serious as is usually associated with the concept of flocculation but sufficient to prevent a fiber from freely rotating into the plane of the network following initial contact. This type of interaction could cause a reduction in the rate of retention. It is largely a matter of speculation but it does not seem logical that an effect of this type would result without an equally serious counterbalancing effect. For example, the fiber whose presence prevents another fiber from freely rotating so as to be retained might by the same interaction be prevented from passing unretained. Other factors such as the acceleration of flow through the slice or the existence of a velocity gradient between the stock and the wire have equally confusing effects. The work of Moss (27) shows that a velocity gradient definitely causes fiber alignment but the effect of such alignment is uncertain. Increased fiber orientation in the direction of flow would result in greater fiber loss but the relative lateral movement of the wire would cause more rapid rotation of the contacting fibers and result in greater fiber retention.

Although the complexities of normal papermaking operations make it impossible to predict from theory the rate of retention on the paper machine, it is possible to make some empirical predictions using Equation (44). As discussed above, Han (22) has demonstrated the applicability of a correlation of this type

to normal sheet-forming operations. An important characteristic of the retention processes treated by this correlation thus far, is that they are continuous. That is, there are no time lags or disruptions such as occur between the table rolls on a fourdrinier machine. The nature of the retention process for each individual table roll would be expected to fit this empirical description. A composite process involving several table rolls might then be described by a suitable extension of this empirical analysis.

In attempting any type of an analysis of the retention process as it applies to the paper machine, care must be taken that the proper variables are being considered. For example, the fiber length distribution to be considered in the conventional sheet-forming system is not that of the original stock but must necessarily be that of the stock suspension which actually is fed onto the wire. The effect of recycling the white water is to shift the effective fiber length distribution to lower values.

Understanding of the dependence of fiber retention upon the important variables of sheet-forming systems might also serve other uses. Knowledge of the dependence of retention upon the fiber length, for example, could provide a useful method for determining average fiber lengths. Such a determination could conceivably involve nothing more than a measurement of the total mass of fibers lost through a screen of known dimensions. From Equations (44) and (46) and the theoretical curves for the rate of initial retention, a set of nomographs could possibly be constructed from which the average fiber length could be determined directly from the measured fiber loss. Other applications might likewise make it possible to determine the fiber length distribution.

With regard to continuing the investigation of ideal systems, there are many factors whose importance could be determined by such simplified studies.

For example, it would be extremely useful to know the relative importance of the different suspension-network interactions mentioned in this work. The importance of such factors as fiber rigidity and width, or the three-dimensional characteristics of woven wires is yet to be determined. Estridge showed that the retention data of Andersson and Bartok (18), obtained using a modified Bauer-McNett classifier, agreed extremely well with the predicted values of initial retention for square-mesh grids. It was necessary to make a correction for the diameter of the wires, but it was found that if the area of the retaining network were simply reduced to the fractional open area of the grid, a good correlation was obtained. This would suggest that fiber width might be dealt with in the same manner. Another related problem worthy of study is in the field of flow resistance. It would be useful to know how the resistance changes from that of the bare grid as retention begins and proceeds. It is already known that fiber mat resistance and wire grid resistance are not directly additive.

CONCLUSIONS

Several conclusions have followed from the observations made throughout the course of this study and have been discussed in some detail above. A summary of a few of the more important conclusions follows.

Through the theoretical treatment of the probability of initial retention by rectangular-mesh grids, it has been demonstrated that the Network Model provides a valid description of the fiber retention process. It is thus no longer necessary to have an explicit description of the geometry of the retaining network in order to predict the rate of fiber retention. It is possible, through the use of random scan-line measurements, to make the evaluations of the network properties necessary for predicting the average retention probability. To make such predictions for actual systems, however, requires some information about the properties of the suspension in addition to knowing the nature of the retaining network. The limitation in this work was found to be the lack of a thorough understanding of the nature of the suspension-network interactions. Because of the inability to take certain suspension-network interactions into account in the application, the Network Model was found to consistently overpredict the rates of fiber retention beyond those of the initial grids. Although quantitative evidence is lacking and the interpretation thus open to question, the suspension-network interaction of greatest influence appears to be the result of the forces exerted upon the retaining network by the depositing fibers. The magnitude and nature of these forces are sufficient to cause the loss of previously retained fibers. Therefore, the net retention rate is lower than predicted from theory.

Through the application of the Network Model to the hypothetical case of fiber retention by a random network, a previously suggested empirical correlation

was derived. This correlation was found to describe the experimental data quite well. The possibility of using this empirical correlation to describe the fiber retention process in normal sheet-forming systems is discussed. It has already been demonstrated that the correlation is applicable in the case of a vacuum former. It would be expected to also be applicable in the case of individual table rolls.

Finally, the possibility is discussed of utilizing the known characteristics of the fiber retention process to develop and apply methods of evaluating other properties. The possible application to average fiber length determinations is discussed specifically.

NOMENCLATURE

A	=	area, $cm.^2$
a	=	grid spacing in X direction, cm. length of linear part of polygonal line, cm.
B	=	dimensionless constant
B_L	=	normalizing factor, 1/cm.
b	=	grid spacing in Y direction, cm.
b'	=	displacement of scan line from central axis, cm.
C	=	constant, 1/cm.
C_1-C_6	=	contribution to frequency distribution of L
D	=	circle diameter, cm.
d_f	=	fiber diameter, cm.
F_D	=	fluid drag force, dynes
F_F	=	force of fiber deposition, dynes
$F(L)$	=	frequency distribution of network distance L
$F(\lambda_1)$	=	frequency distribution of network distance λ_1
$F(\lambda_1 \mid L)$	=	conditional frequency distribution of λ_1 on L
$F(n)$	=	binomial distribution of n
$F(S)$	=	frequency distribution of S
H	=	dimensionless constant
K	=	constant, $cm.^2/g.$
L	=	network distance, cm.
$\bar{L}$	=	average network distance, cm.
$\bar{L}_o$	=	initial average network distance, cm.
L_f	=	fiber length, cm.
L_p	=	perimeter of polygonal line, cm.
L_s	=	length of scan line, cm.

N = number of random trials
number of intersections between scan line and network

N_f = number of fiber centers in area A

N_i = number of approaching fibers (ith type)

N_s = number of intersections with scan line

$\bar{N}_s$ = expected number of scan-line intersections

N_t = total number of approaching fibers

n = number of successes in N random trials

$\bar{n}$ = expectation value of n

n_a = number of linear parts of a polygonal line

n_i = number of fibers (ith type) retained

n_t = total number of fibers retained

P = probability that an event will occur

P_i = probability of retention for ith-type fiber

$\bar{P}_i$ = average of P_i over area A

p_i = probability of intersection with scan line

R = mass fraction retained

R_o = initial mass fraction retained

r_d = rate of deceleration, cm./sec.^{2}

S = $\sin(\theta)$

T_1-T_6 = random numbers

U = superficial velocity, cm./sec.

u = variable equal to 1 or 0, depending upon whether intersection does or does not occur with scan line

$\bar{u}$ = expected value of u

V_r = value of W_r when W_t V_t

V_t = value of the total approaching fiber mass

W_p = total mass of fibers passed unretained throughout entire retention process, g.

$\underline{W}_{\underline{r}}$ = mass of fiber retained, g.

$\underline{W}_{\underline{t}}$ = total approaching mass of fibers, g.

$\underline{w}$ = mass of fiber per unit length, g./cm.

$\underline{X}$ = co-ordinate, axes

$\underline{x}$ = distance in $\underline{X}$ direction, cm.

$\underline{x}_{\underline{c}}$ = $\underline{x}$ co-ordinate of fiber center, cm.

$\underline{Y}$ = co-ordinate, axes

$\underline{y}$ = distance in $\underline{Y}$ direction, cm.

$\underline{y}_{\underline{c}}$ = $\underline{y}$ co-ordinate of fiber center, cm.

$\underline{Z}$ = co-ordinate, axes

$\underline{z}$ = distance in $\underline{Z}$ direction, cm.

$\underline{z}_{\underline{c}}$ = $\underline{z}$ co-ordinate of fiber center, cm.

α = $\underline{L} - \underline{b}/\sin(\theta)$

γ = $\underline{L} - \underline{a}/\cos(\theta)$

ϵ = porosity, dimensionless

ζ_o = length of grid per unit area, 1/cm.

$\zeta_{\underline{f}}$ = length of fiber per unit area, 1/cm.

θ = angle of co-latitude, radians

λ_1 = network distance, cm.

λ_2 = network distance, cm.

μ = fluid viscosity, poises

ρ = fiber density, g./cc.

$\sigma_{\underline{i}}$ = mass per fiber ($\underline{i}$th type), g.

$\bar{\sigma}$ = average mass per fiber in the approaching suspension, g.

$\bar{\sigma}_{\underline{r}}$ = average mass of fibers retained, g.

ϕ = azimuth angle, radians

$\phi_{\underline{c}}$ = angle of concentrated frequency of L, radians

$\phi_{\underline{s}}$ = random scanning angle, radians

ACKNOWLEDGMENTS

The author wishes to give special credit to a few individuals whose assistance was of particular importance to the successful completion of this study. Mr. S. T. Han, chairman of the thesis advisory committee, and Dr. W. L. Ingmanson and Dr. R. W. Nelson, also members of the advisory committee, are to be thanked for lending their advice and encouragement when it was most needed. In addition, the author is deeply indebted to Dr. Nelson for lending his assistance in the development of the mathematics of the Network Model and for supplying the derivation of the distance distribution for rectangular networks.

Credit is also given to Mr. F. R. Sweeney of the Photography Department of The Institute of Paper Chemistry for assisting in the development of the photographic techniques, to the members of the Electrical, Machine, and Millwright Shops of The Institute of Paper Chemistry for assisting in the construction of the apparatus, to Mr. B. D. Andrews and Mr. O. C. Kuehl of the Engineering and Technology Section of the Institute for assisting throughout the experimental phase of the work, to Mrs. Sharon Abrams, the author's wife, for assisting in the analysis of the network photographs and for offering continued encouragement, and to Mrs. Elizabeth Cary for assisting in the preparation of this manuscript.

LITERATURE CITED

1. Corte, H. The porous structure of paper. In Bolam's Fundamentals of papermaking fibres. p. 301-31. Kenley, England, Tech. Sect. Brit. Paper and Board Makers' Assoc., 1958.

2. Kallmes, O., and Corte, H., Tappi 43, no. 9:737-52(1960).

3. Kallmes, O., Corte, H., and Bernier, G., Tappi 44, no. 7:519-28(1961).

4. Kallmes, O., and Bernier, G., Tappi 45, no. 11:867-72(1962).

5. Kallmes, O., and Bernier, G., Tappi 46, no. 2:108-14(1963).

6. Kallmes, O., Corte, H., and Bernier, G., Tappi 46, no. 8:493-502(1963).

7. Corte, H., and Kallmes, O. Statistical geometry of a fibrous network. In Bolam's The formation and structure of paper. p. 13-46. London, England, Tech. Sect. Brit. Paper and Board Makers' Assoc., 1962.

8. Van den Akker, J. A. Some theoretical considerations on the mechanical properties of fibrous structures. In Bolam's The formation and structure of paper. p. 205-41. London, England, Tech. Sect. Brit. Paper and Board Makers' Assoc., 1962.

9. Page, D. H., and Tydeman, P. A. A new theory of the shrinkage, structure, and properties of paper. In Bolam's The formation and structure of paper. p. 397-413. London, England, Tech. Sect. Brit. Paper and Board Makers' Assoc., 1962.

10. Bliesner, W. C. A study of the porous structure of fibrous sheets using permeability techniques. Doctor's Dissertation. Appleton, Wisconsin, The Institute of Paper Chemistry, 1963. 216 p.

11. Majewski, Z. J. Effect of forming processes on sheet structure. In Bolam's The formation and structure of paper. p. 749-66. London, England, Tech. Sect. Brit. Paper and Board Makers' Assoc., 1962.

12. Andersson, O., and Steen, I. Influence of suspension nonuniformity on sheet structure. In Bolam's The formation and structure of paper. p. 771-82. London, England, Tech. Sect. Brit. Paper and Board Makers' Assoc., 1962.

13. Johnson, R. C. A study of particle retention in relation to the structure of a fibrous mat. Doctor's Dissertation. Appleton, Wis., The Institute of Paper Chemistry, 1962. 99 p.; Tappi 46, no. 5:304-8(May, 1963).

14. Estridge, R. The initial retention of fibers by wire grids. Doctor's Dissertation. Appleton, Wis., The Institute of Paper Chemistry, 1961. 129 p.; Tappi 45, no. 4:285-91(April, 1962).

15. Steenberg, B., and Kubat, J., Svensk Papperstid. 58, no. 9:319-24(May, 1955).

16. Kubat, J., Svensk Papperstid. 59, no. 5:175-8(March, 1956).

17. Kubat, J., Svensk Papperstid. 59, no. 7:251-6(April, 1956).

18. Andersson, O., and Bartok, W., Svensk Papperstid. 58, no. 10:367-73(May, 1955).

19. Nelson, R. W. Personal communication, 1962.

20. Davies, O. L. Statistical methods in research and production. 3d ed. p. 274. New York, Hafner Publishing Company, 1957.

21. Jaeger, J. C. An introduction to applied mathematics. p. 37. London, Oxford University Press, 1956.

22. Han, S. T., Tappi 45, no. 4:292-5(April, 1962).

23. Arnold, E. W. Light scattering in fibrous sheets. Doctor's Dissertation. Appleton, Wis., The Institute of Paper Chemistry, 1962. 139 p.

24. Mason, S. G., Tappi 37, no. 11:494-501(Nov., 1954).

25. Hodgman, C. D., Ed. C. R. C. standard mathematical tables. 12th ed. p. 238. Cleveland, O., Chemical Rubber Publishing Co., 1962.

26. Parker, J. D., Tappi 44, no. 4:162A-7A(April, 1961).

27. Moss, L. A. A photographic study of fibers and water in flowing fiber suspensions. Doctor's Dissertation. Appleton, Wis., The Institute of Paper Chemistry, 1937. 159 p.

28. Andrews, B. D. Personal communication, 1963.

29. Ingmanson, W. L. Personal communication, 1961.

30. Jentzen, C. A. The effect of stress applied during drying on the mechanical properties of individual pulp fibers. Doctor's Dissertation. Appleton, Wis., The Institute of Paper Chemistry, 1964. 129 p.

31. Uspensky, J. V. Introduction to mathematical probability. p. 253. New York, McGraw-Hill, 1937.

32. Happel, J., A.I.Ch.E. Journal 5, no. 2:174-7(June, 1959).

APPENDIX I

DERIVATION OF THE SCAN-LINE RELATIONSHIP

The probable number of intersections of a randomly oriented straight line with members of a two-dimensional fiber network is

$$N = 2L_s N_f L_f / \pi A \qquad (49),$$

where L_s is the length of the scan line and N_f is the total number of fiber centers in area A. The derivation which Kallmes and Corte (2) gave for this equation imposes the limitation that the network must be random with respect to both fiber position and fiber orientation in the same sense as defined above. That is, the distributions of fiber centers and of fiber orientations must be random and uniform. The equation can be shown to be more generally applicable, however, by deriving it under less restrictive conditions. The following derivation is similar to Barbier's solution of Buffon's Needle Problem (31).

Consider a polygonal line thrown upon an area A which contains a randomly oriented scan line of length L_s. It is desired to know the expected number of intersections between the two lines. The perimeter of the polygonal line can be divided into n_a linear parts, $a_1, a_2, a_3 \ldots, a_i \ldots, a_n$. With these n_a parts are associated n_a variables, $u_1, u_2, u_3 \ldots, u_i \ldots, u_n$, such that

u_i = 1, if the scan line intersects a_i;

u_i = 0, otherwise.

The total number of intersections is then given by the sum

$$N_s = u_1 + u_2 + u_3 + \ldots + u_i + \ldots + u_n \qquad (50).$$

The expected number of intersections is, then,

$$\bar{N}_s = \bar{u}_1 + \bar{u}_2 + \bar{u}_3 + \ldots + \bar{u}_i + \ldots + \bar{u}_n \qquad (51).$$

If p_i is the probability of intersection of a_i with the scan line,

$$\bar{u}_i = p_i \qquad (52).$$

And if p_i is directly proportional to the length of a_i,

$$p_i = Ca_i \qquad (53),$$

where C is a constant independent of length. In general, therefore,

$$\bar{N}_s = C(a_1 + a_2 + a_3 + \ldots + a_i + \ldots + a_n) = CL_p \qquad (54),$$

where L_p is the perimeter of the polygonal line.

For the special case of a circle of diameter A/L_s, $\bar{N}_s = 2$, since such a circle has always exactly two points of intersection. Therefore,

$$C = 2L_s/\pi A \qquad (55),$$

and

$$\bar{N}_s = CL_p = 2L_sL_p/\pi A \qquad (56).$$

A number of fibers can be connected by such a polygonal line such that it passes along the axis of each individual fiber. The number of intersections of fibers with the scan line is then related to the number of intersections of the entire line with the scan line as their relative lengths are related. Therefore,

$$N/\bar{N}_s = N_fL_f/L_p \qquad (57),$$

where N is the number of intersections with fibers, N_f is the total number of

fibers, and $\underline{L_f}$ is the individual fiber length. Therefore,

$$N = \bar{N}_s N_f L_f / L_p = 2 L_s N_f L_f / \pi A \qquad (58).$$

The average distance between intersections can now be defined as

$$\bar{L} = L_s / N = A / 2 N_f L_f = \pi / 2 \zeta_f \qquad (59)$$

where $\underline{\zeta_f}$ is the total length of fiber per unit area. A simple modification of this equation results in Equation (40).

APPENDIX II

EXPERIMENTAL DATA

TABLE VII

FIBER LENGTH DISTRIBUTIONS

Length Interval, cm. x 10	Number of Fibers Counted					
1.2-2.3	2					
1.3-1.4	5					
1.4-1.5	116					
1.5-1.6	109					
1.6-1.7	9					
1.9-2.0		4				
2.0-2.1		66				
2.1-2.2		139				
2.2-2.3		65				
2.3-2.4		4				
2.6-2.7						15
2.7-2.8			2			48
2.8-2.9			20			60
2.9-3.0			68			33
3.0-3.1			61			9
3.1-3.2			32			
3.2-3.3			5			
3.4-3.5				1		
3.5-3.6				36		
3.6-3.7				79		
3.7-3.8				79		
3.8-3.9				30		
3.9-4.0				2		
4.8-4.9					8	
4.9-5.0					22	
5.0-5.1					40	
5.1-5.2					34	
5.2-5.3					23	
5.3-5.4					4	
1.2-5.4	241	278	188	236	131	165
Av. length, cm.	0.150	0.215	0.301	0.370	0.509	0.283

TABLE VIII

FIBER RETENTION MASS DATA

Run 1
a = 0.356 cm.
b = 0.356 cm.
L_f = 0.370 cm.

$(W_t/A)\times10^4$, g./cm.^{2}	$(W_r/A)\times10^4$, g./cm.^{2}
0.63	0.00
2.71	0.34
5.00	0.68
7.02	1.24
9.13	1.99
11.32	2.97
13.59	4.26
15.83	5.66
18.05	7.33
20.39	9.25
23.00	11.48
26.43	14.62
30.82	18.72
35.19	22.84
40.07	27.50
46.30	33.52

Run 2
a = 0.356 cm.
b = 0.356 cm.
L_f = 0.370 cm.

$(W_t/A)\times10^4$, g./cm.^{2}	$(W_r/A)\times10^4$, g./cm.^{2}
1.08	0.03
3.69	0.31
6.44	0.83
8.89	1.56
11.36	2.58
14.12	4.11
16.96	6.07
20.04	8.40
22.71	10.74
26.18	13.85
29.21	16.64
32.16	19.42
36.08	23.16
40.23	27.13

Run 3
a = 0.254 cm.
b = 0.254 cm.
L_f = 0.283 cm.

$(W_t/A)\times10^4$, g./cm.^{2}	$(W_r/A)\times10^4$, g./cm.^{2}
1.75	0.02
6.55	1.15
10.94	2.71
18.50	6.71
24.79	11.28
31.43	16.91
40.44	25.15
49.38	33.67
62.72	46.54
76.58	60.03
91.29	74.37

Run 4
a = 0.254 cm.
b = 0.254 cm.
L_f = 0.283 cm.

$(W_t/A)\times10^4$, g./cm.^{2}	$(W_r/A)\times10^4$, g./cm.^{2}
1.20	0.06
4.14	0.72
6.70	1.43
9.32	2.26
12.27	3.47
15.22	4.93
18.03	6.55
21.60	8.94
25.06	11.58
28.50	14.46
31.82	17.32
35.70	20.77
38.70	23.50
44.70	29.14

Run 5
a = 0.127 cm.
b = 0.127 cm.
L_f = 0.150 cm.

$(W_t/A)\times10^4$, g./cm.^{2}	$(W_r/A)\times10^4$, g./cm.^{2}
1.19	0.05
3.85	0.53
6.51	1.07
9.12	1.67
12.06	2.55
14.64	3.56
17.47	4.81
20.89	6.76
23.68	8.54
27.47	11.31
30.85	14.04
35.14	17.81
41.62	23.74
47.97	29.78
53.51	35.14

Run 6
a = 0.254 cm.
b = 0.254 cm.
L_f = 0.301 cm.

$(W_t/A)\times10^4$, g./cm.^{2}	$(W_r/A)\times10^4$, g./cm.^{2}
3.55	0.69
6.57	1.62
9.78	3.07
13.03	4.76
16.35	6.98
21.37	11.00
25.07	14.23
29.78	18.55
34.04	22.52
40.10	28.36
47.45	35.44
53.00	40.83
55.80	43.53

TABLE VIII (Continued)

Run 7
a = 0.178 cm.
b = 0.178 cm.
L_f = 0.215 cm.

$(W_t/A)\times10^4$, g./cm.^{2}	$(W_r/A)\times10^4$, g./cm.^{2}
1.55	0.15
4.67	0.89
7.62	1.76
10.37	2.75
12.98	3.80
15.69	5.13
18.74	6.85
22.21	9.04
25.19	11.25
28.98	14.18
32.48	17.12
35.63	19.55
39.48	22.88
44.19	26.89
53.84	35.28

Run 8
a = 0.356 cm.
b = 0.356 cm.
L_f = 0.509 cm.

$(W_t/A)\times10^4$, g./cm.^{2}	$(W_r/A)\times10^4$, g./cm.^{2}
0.36	0.00
3.59	2.00
7.39	5.24
10.70	8.32
14.63	12.04
22.11	19.19
27.18	24.07
34.56	31.24
43.93	40.36
53.61	49.85
64.10	60.15

Run 9
a = 0.254 cm.
b = 0.254 cm.
L_f = 0.370 cm.

$(W_t/A)\times10^4$, g./cm.^{2}	$(W_r/A)\times10^4$, g./cm.^{2}
0.33	0.07
2.11	0.85
3.86	1.85
5.52	2.87
7.18	4.13
9.35	5.99
11.11	7.54
13.54	9.72
15.43	11.48
18.81	14.64
23.22	18.82
28.76	24.18

Run 10
a = 0.254 cm.
b = 0.254 cm.
L_f = 0.370 cm.

$(W_t/A)\times10^4$, g./cm.^{2}	$(W_r/A)\times10^4$, g./cm.^{2}
1.37	0.47
3.53	1.65
5.84	3.27
7.90	5.01
9.85	6.62
12.52	9.00
15.80	12.02
21.56	17.47
25.17	20.93

Run 11
a = 0.178 cm.
b = 0.178 cm.
L_f = 0.283 cm.

$(W_t/A)\times10^4$, g./cm.^{2}	$(W_r/A)\times10^4$, g./cm.^{2}
0.81	0.36
3.49	2.03
6.23	3.99
9.01	6.21
14.30	10.83
22.11	18.19
30.70	26.39
50.12	45.28

Run 12
a = 0.178 cm.
b = 0.178 cm.
L_f = 0.301 cm.

$(W_t/A)\times10^4$, g./cm.^{2}	$(W_r/A)\times10^4$, g./cm.^{2}
0.90	0.49
2.96	1.86
5.53	3.91
9.73	7.52
11.96	9.56
14.29	11.74
16.51	13.86
25.63	22.59
36.70	33.27

TABLE VIII (Continued)

Run 13
a = 0.178 cm.
b = 0.178 cm.
L_f = 0.301 cm.

$(W_t/A)\times10^4$, g./cm.^{2}	$(W_r/A)\times10^4$, g./cm.^{2}
0.38	0.18
1.80	1.08
3.30	2.08
5.28	3.53
7.19	5.06
9.73	7.23
11.67	8.97
16.55	13.57
20.94	17.72
25.07	21.65

Run 14
a = 0.127 cm.
b = 0.127 cm.
L_f = 0.215 cm.

$(W_t/A)\times10^4$, g./cm.^{2}	$(W_r/A)\times10^4$, g./cm.^{2}
1.05	0.37
4.79	2.65
8.10	4.89
10.95	7.10
14.08	9.73
17.39	12.71
21.17	16.22
28.74	23.37
36.70	31.04
46.04	40.09
52.92	46.78
61.10	54.80

Run 15
a = 0.254 cm.
b = 0.254 cm.
L_f = 0.509 cm.

$(W_t/A)\times10^4$, g./cm.^{2}	$(W_r/A)\times10^4$, g./cm.^{2}
0.18	0.09
1.81	1.36
3.58	2.86
5.61	4.73
7.78	6.74
10.95	9.68
14.11	12.69
18.56	16.93
22.74	20.96
28.17	26.20

Run 16
a = 0.127 cm.
b = 0.127 cm.
L_f = 0.283 cm.

$(W_t/A)\times10^4$, g./cm.^{2}	$(W_r/A)\times10^4$, g./cm.^{2}
0.58	0.46
2.37	1.97
3.81	3.20
5.50	4.67
7.41	6.34
10.33	8.99
13.21	11.67
19.29	17.45
24.85	22.78
28.97	26.74

Run 17
a = 0.127 cm.
b = 0.127 cm.
L_f = 0.301 cm.

$(W_t/A)\times10^4$, g./cm.^{2}	$(W_r/A)\times10^4$, g./cm.^{2}
0.00	0.00
1.19	1.10
2.57	2.30
3.77	3.28
4.94	4.31
6.14	5.40
7.39	6.54
11.93	10.79
15.89	14.60
22.86	21.29
27.33	25.58

Run 18
a = 0.178 cm.
b = 0.356 cm.
L_f = 0.301 cm.

$(W_t/A)\times10^4$, g./cm.^{2}	$(W_r/A)\times10^4$, g./cm.^{2}
0.87	0.24
2.58	0.93
4.19	1.70
5.93	2.74
7.43	3.56
9.11	4.76
10.64	5.93
12.38	7.35
14.28	8.94
16.24	10.64
18.47	12.67
20.80	14.81
24.07	17.83
26.72	20.32

TABLE VIII (Continued)

Run 19
a = 0.178 cm.
b = 0.356 cm.
L_f = 0.370 cm.

$(W_t/A)\times10^4$, g./cm.^{2}	$(W_r/A)\times10^4$, g./cm.^{2}
0.45	0.19
1.82	1.11
3.25	2.04
4.57	3.03
6.14	4.25
7.83	5.65
10.01	7.58
13.01	10.34
16.27	13.39
19.27	16.23
22.85	19.62
25.13	21.79

Run 20
a = 0.178 cm.
b = 0.356 cm.
L_f = 0.509 cm.

$(W_t/A)\times10^4$, g./cm.^{2}	$(W_r/A)\times10^4$, g./cm.^{2}
0.43	0.28
1.88	1.43
3.33	2.67
4.79	3.94
6.43	5.41
8.10	6.96
11.71	10.34
16.44	14.87
20.01	18.30
24.26	22.44

Run 21
a = 0.127 cm.
b = 0.381 cm.
L_f = 0.301 cm.

$(W_t/A)\times10^4$, g./cm.^{2}	$(W_r/A)\times10^4$, g./cm.^{2}
0.48	0.22
1.96	1.14
3.32	1.98
4.86	3.10
6.31	4.22
7.98	5.57
9.71	7.05
12.83	9.90
16.00	12.81
19.75	16.32
25.27	21.56

Run 22
a = 0.127 cm.
b = 0.381 cm.
L_f = 0.370 cm.

$(W_t/A)\times10^4$, g./cm.^{2}	$(W_r/A)\times10^4$, g./cm.^{2}
1.47	0.90
2.71	1.86
4.03	2.95
5.27	4.04
6.72	5.33
8.66	7.12
10.69	8.98
14.17	12.28
18.52	16.45
22.54	20.31

Run 23
a = 0.127 cm.
b = 0.381 cm.
L_f = 0.509 cm.

$(W_t/A)10^4$, g./cm.^{2}	$(W_r/A)\times10^4$, g./cm.^{2}
0.46	0.32
1.55	1.23
2.71	2.26
3.71	3.17
4.80	4.14
7.12	6.32
10.08	9.13
13.51	12.43
19.00	17.72

APPENDIX III

RELATIVE MAGNITUDES OF FLUID DRAG AND FIBER DEPOSITION FORCES

The fluid drag force for flow perpendicular to the major axis of a cylindrical fiber can be determined from the equation of Happel (32),

$$F_D = 4\pi\mu U L_f / \left\{ \ln[(1-\epsilon)^{-1/2}] - [1-(1-\epsilon)^2]/2[1+(1-\epsilon)^2] \right\} \qquad (60),$$

where μ is the viscosity of the fluid, U is the superficial velocity, and ϵ is the porosity of the fiber system. Assuming the fibers to lie in a single plane, the porosity is given by

$$\epsilon = 1 - \pi\zeta_f d_f/4 = W_r/\rho d_f \qquad (61)$$

where ρ is the fiber density. For a network of nylon fibers 4.1×10^{-3} cm. in diameter and a mass per unit area of 5×10^{-4} g./cm.^{2}, ϵ is equal to 0.96. For water flowing at a superficial velocity of 4 cm./sec. and a temperature of 30°C., the fluid drag force per unit length of fiber is 0.33 dyne. For a fiber 0.3 cm. long, the fluid drag force would be approximately 0.1 dyne. In comparison to the force of fluid drag, the gravitational force on the fiber is negligible, being approximately 4.5×10^{-3} dynes.

If it is assumed that a fiber coming into contact with the retaining network decelerates uniformly to a position of rest, it can be shown from the laws of motion that the rate of deceleration is

$$r_d = U^2/2\Delta z \qquad (62),$$

where Δz is the distance the fiber center travels from the time of initial contact to the time of rest. The force between the fiber and the retaining network is the product of the rate of deceleration and the fiber mass,

$$F_F = \sigma r_d = \pi \rho U^2 d_f^2 L_f / 8 \Delta z \qquad (63).$$

For a 0.3-cm. long fiber approaching at a 45° angle to the plane of the network and making initial contact at a point 0.1 cm. from its leading end, Δz is equal to 0.035 cm. Under the same flow conditions as above, the force of deposition is approximately 1×10^{-3} dynes. If the angle of approach is reduced from 45 to 10°, the force is increased to 4×10^{-3} dynes. It is apparent that the force of deposition is negligible compared with the fluid drag force. However, the depositing fiber is also experiencing the force of fluid drag which is additive with the force of deposition. It is reasonable to assume, therefore, that the net difference in force experienced by a fiber in the network, when contacted by a depositing fiber, is of the same order of magnitude as the fluid drag force.

The relative magnitudes of the two forces, however, is not the only factor of importance. There is a major difference in the manner in which the two forces act upon the network fiber. The fluid drag force is distributed uniformly along the length of the fiber, whereas the force imparted by a depositing fiber is concentrated at the point of contact. Therefore, the force of impact could appreciably alter the over-all mass balance within the structure of the network.